Integration of phononic metamaterials in aircraft structures

An exploratory research on Helmholtz resonator-based metamaterial structures

Petre Calin Nae

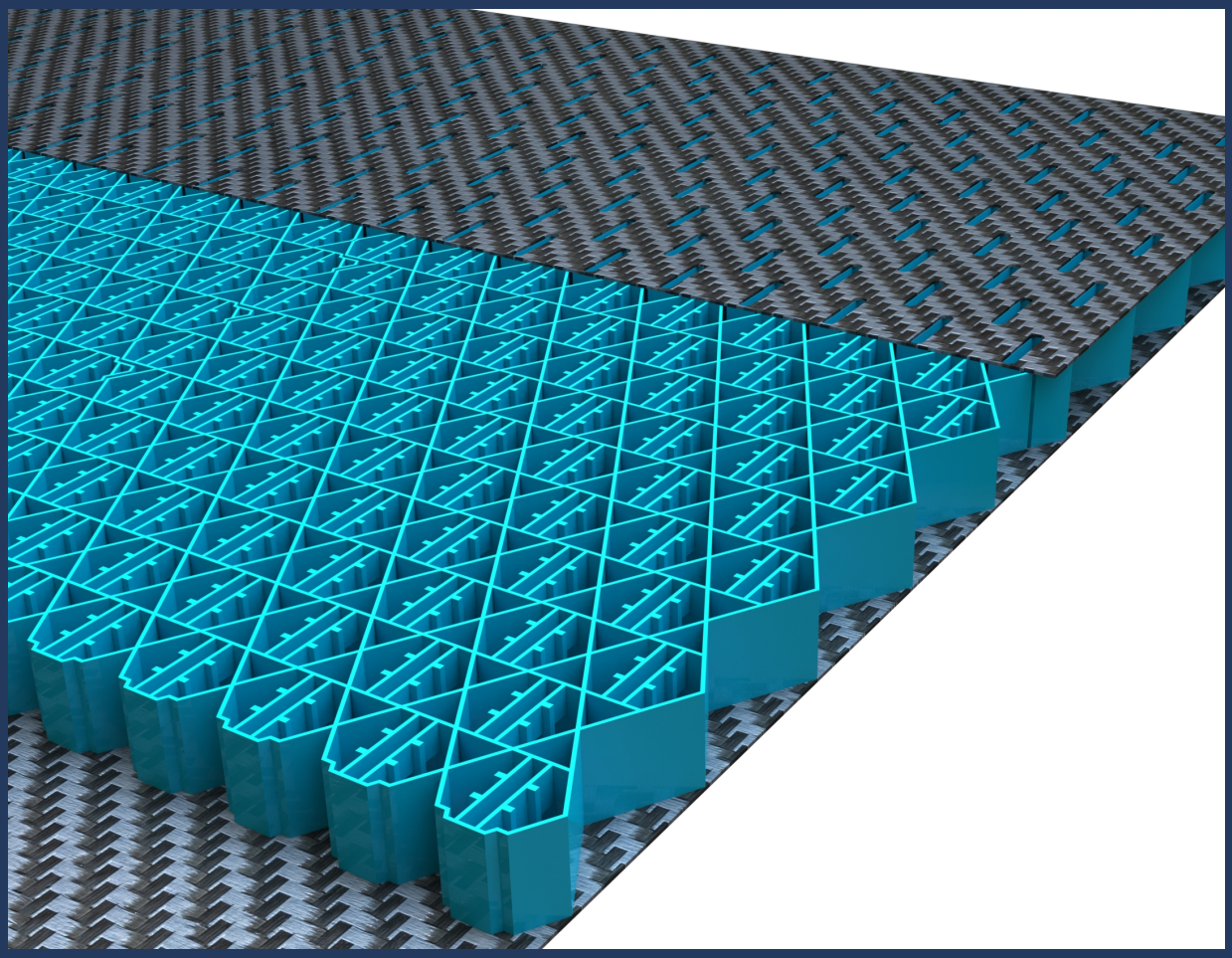

TU Delft

Integration of phononic metamaterials in aircraft structures

An exploratory research on Helmholtz resonator-based metamaterial structures

by

Petre Calin Nae

to obtain the degree of Master of Science
at the Delft University of Technology
to be defended publicly on August 5, 2024 at 14:00

Student Number:	4535650	
Thesis committee:	Dr. J.A. Pascoe	TU Delft, Chair
	Dr. J. Jovanova	TU Delft, Examiner
	Dr. K. Masania	TU Delft, Supervisor
	Dr. S. Sharma	TU Delft, Mentor

An electronic version of this thesis is available at http://repository.tudelft.nl/.

TU Delft

Acknowledgements

I want to express my deepest gratitude to my supervisor, Dr Kunal Masania, for his invaluable guidance, support, and encouragement throughout this research. His insights and expertise have been instrumental in shaping this thesis, and his constant support has been a source of great motivation. Dr Masania's constructive feedback and advice have greatly improved this work's quality, and I deeply appreciate the time and effort he has invested in my academic development.

I would also like to extend my special thanks to the technicians at DASML for their technical assistance and support. Their expertise and dedication have been crucial in completing the experimental work presented in this thesis. The willingness of DASML technicians to assist with any challenges that arose and their commitment to excellence have been greatly appreciated. Their support in the laboratory and with the equipment has been invaluable.

Reflecting on my academic journey at TU Delft, pursuing a Master's in Aerospace Engineering with a focus on Materials and Structures, I recognise the significant growth and learning I have experienced. This journey has been both challenging and rewarding. One of the major challenges I faced was finding the right writing form for this thesis. The process of articulating complex ideas and presenting them coherently and academically rigorously was demanding. Despite these difficulties, the struggle with writing has taught me perseverance and the importance of clear communication in academic research.

In contrast, I found immense enjoyment and fulfilment in the practical aspects of this research, including designing, manufacturing, and testing. These hands-on experiences have been the highlight of my academic journey. Working on the practical aspects allowed me to apply theoretical knowledge to real-world problems, which was exciting and educational. Creating, testing, and refining designs was deeply satisfying and reinforced my passion for engineering and innovation.

I am also grateful to my fellow students and colleagues at TU Delft, who have provided a supportive and stimulating environment. The collaborative spirit and intellectual exchanges with peers have enriched my learning experience and have been a source of inspiration.

Lastly, I thank my family and friends for their unwavering support and encouragement throughout my studies. Their understanding, patience, and belief in my abilities have constantly strengthened and motivated me. Their support has been essential, particularly during the more challenging times of this journey.

This work would not have been possible without the contributions and support of all these individuals and institutions. I am deeply thankful for the guidance, assistance, and encouragement I have received.

Thank you.

P.C. Nae
Delft, August 2024

Abstract

The aviation industry is constantly pursuing enhancing passenger comfort and safety, with noise reduction within aircraft cabins being a critical area of focus. Traditional soundproofing methods, often involving the addition of heavy and voluminous materials, conflict with the industry's goal of maintaining lightweight aircraft and minimising fuel consumption. Previous research suggests that Helmholtz resonators offer a promising approach to noise control. Their simple structure, consisting of an enclosed volume connected to the external environment through an aperture, allows for customisable and scalable noise control applications.

The thesis presents exploratory research into integrating Helmholtz resonator-based metamaterials into lightweight composite acoustic sandwich panels for aircraft cabins. First, the stiffness of the resonator's enclosure is investigated, followed by determining the effects of placing the inlet within the resonance chamber. Next, the implications of creating resonators for single-layer acoustic sandwich panels are studied. Finally, three reinforcement fibres are investigated for acoustic suitability: fibreglass, carbon fibre and flax fibre. The study concludes with a weight comparison between the developed metamaterial sandwich panel and commercial designs.

The findings reveal that the lay-up of the face sheets significantly affects sound absorption. Introducing non-resonant volumes between the metamaterial's unit cells is the most effective method to prevent interference between the resonators. The resonator's inlet disrupts the stress flow in one of the face sheets, leading to locally increased stress values. The need for specific acoustic properties requires core cell sizes larger than those typically used in standard cabin panels, compromising the stability of the face sheets. Support columns are proposed as a solution, lessening the impact on stability. The thesis proves that lightweight composite single-layer acoustic panels are achievable by incorporating Helmtolhtz resonator-based phononic metamaterials.

Contents

List of Figures

List of Tables

1

Introduction

Passenger safety and comfort remain paramount in the aviation industry. Aircraft manufacturers strive to enhance the flying experience through more comfortable designs while adhering to zero-emission requirements set by the International Civil Aviation Organization (ICAO).

Noise significantly contributes to discomfort in air travel. Comfortable noise levels are generally between 30 to 50 dB, allowing for conversation. Disturbing noise levels begin above 70 dB, with prolonged exposure leading to discomfort, fatigue, and hearing loss. Noise levels above 85 dB can significantly impact human comfort and well-being. During cruise, commercial aircraft cabin noise levels typically range from 75 to 85 dB. Business and corporate jets aim for lower noise levels, often around 70 to 75 dB, with soundproofing treatments targeting ”library quiet” levels of around 40 dB in bedroom zones.

Current commercial solutions enhance sound absorption by adding porous materials, such as foams and felt, to the backside of cabin elements and applying barriers through rubberised membranes. While effective in sound absorption, these dense porous materials add significant weight and impact cabin volume, leading to higher fuel consumption, increased emissions, and substantial maintenance burdens.

The aviation industry needs a different approach to soundproofing, focusing on enhancing existing structures’ intrinsic sound absorption properties instead of adding dedicated soundproofing materials. Phononic metamaterials offer a promising alternative for addressing soundproofing challenges. These engineered materials exhibit unique acoustic properties due to their structural topology rather than their base materials.

Phononic metamaterials specifically target sound waves, enabling sound control, direction, and manipulation in ways traditional materials cannot. The structural approach allows them to display remarkable properties such as negative refractive indices and cloaking effects, enhancing their ability to absorb sound and reduce noise transmission. Recent advancements in phononic metamaterials have led to innovative designs that significantly improve sound absorption and isolation.

A Helmholtz resonator, a standard unit in phononic metamaterials, consists of an enclosed volume connected to the external environment through a small opening or neck. When exposed to a sound field, the air within the resonator vibrates at specific frequencies, resulting in sound absorption at the resonance frequency. Tuning unit cells to different frequencies broadens the metamaterial’s bandwidth. Helmholtz resonators effectively target specific frequencies, making them invaluable for applications requiring precise sound control.

Helmholtz resonator arrays use multiple resonators tuned to different frequencies to create broad-spectrum sound absorption. Arranging resonators in specific patterns achieves high levels of sound attenuation across a wide range of frequencies. However, inadequate wall stiffness in the resonator chambers can lead to cross-talk, where resonators interfere, compromising the sound absorption performance. This highlights the need to optimise the design and construction of Helmholtz resonator-based metamaterial arrays.

Cabin lining is a prime candidate for phononic metamaterials. This component closely follows the fuselage contour and acts as a barrier between the occupants and the rest of the aircraft skin. Due to its proximity to the passengers, it must withstand the fuselage's cyclical loading and remain unaffected by the crash and flight envelope loads. Innovative soundproofing solutions that minimally impact an aircraft's weight are crucial for passenger comfort, fuel efficiency, and reducing emissions.

By improving existing structures' intrinsic sound absorption properties, the industry can create quieter and more comfortable cabins across various modes of transportation without the drawbacks of current commercial solutions. Phononic metamaterials, especially those utilising Helmholtz resonators, present a promising avenue for achieving these goals while meeting ICAO's zero-emission requirements.

2

Literature Review

This chapter presents a literature review that delves into the origins of metamaterials, the noise sources and levels encountered within commercial aircraft, the sound mitigation strategies currently in place and state-of-the-art research on various types of phononic metamaterials to identify the most suitable metamaterial unit cells and the gaps in its understanding.

The term ”metamaterial” was initially defined within the electromagnetic domain. Wieglhofer and Lakhtakia [1] described it as a three-dimensional, periodic cellular structure designed to produce optimised responses unavailable in natural materials. Cui, Liu, and Smith [2] expanded this definition to encompass macroscopic composites whose properties arise from their structural and chemical composition. Metamaterials derive their unique characteristics primarily from their geometry and arrangement rather than their composition, enabling properties rarely found in naturally occurring materials.

In acoustics, metamaterials gained momentum following Veselago’s [3] theoretical demonstration and Pendry’s [4] experimental realisation of negative refraction, which paved the way for innovations in acoustic control. Phononic metamaterials are engineered materials that control acoustic and elastic waves through their unique properties, such as negative effective mass density and modulus. These metamaterials are periodic structures that create bandgaps: frequency ranges where wave propagation is prohibited. Like electronic bandgaps in semiconductors, this effect allows precise control over acoustic waves. The bandgaps can be tailored to specific frequencies by altering geometry and material composition, making phononic metamaterials highly versatile for aerospace applications.

2.1. Aircraft cabin noise

The following section provides an overview of the noise sources within the aircraft cabin. Additionally, it presents the levels of noise experienced by passengers during standard commercial flights, with a specific focus on a flight aboard a Boeing 787 as a case study.

2.1.1. Sources of noise in aircraft

The cabin interior noise is due to multiple sources. External, such as the engines, propellers, and turbulent boundary layer, or internal, such as the air-conditioning system or hydraulic systems [5]. The turbulent boundary layer is the primary source of noise during the cruise phase of flight and the primary source of broadband noise. The aerodynamic noise is transmitted inside the cabin if the turbulent layer’s convection speed matches the fuselage skin’s flexural wave speed [6].

Sound transmission occurs due to the jet exhaust interacting with the fuselage. The noise spectrum is constant along an extensive range of frequencies, with peaks depending on the location along the fuselage. Fan noise is created due to the blade passage frequency and pure tones produced by the shock waves encountered in the supersonic flow region of the fan blades [7]. Finally, engine vibrations are created due to minute out-of-balance forces exciting the surrounding structure. Aircraft with the engines mounted in the

aft are most affected by this source, as the engines are connected directly to the fuselage, resulting in structure-borne sound [5].

2.1.2. Noise levels in modern airliners

The A-weighted decibel level (dB(A)) is commonly used to represent sound levels in environmental noise measurements and occupational health and safety standards. This scale approximates the human ear's response to moderate to high sound frequencies, attenuating low and high-frequency sounds while emphasising mid-range frequencies relevant to human hearing.

The noise levels in narrow and wide-body aircraft were analysed in the literature. Wide-body aircraft like the B787 experience lower noise levels than their regional counterparts. This is due to the longer flight duration and greater need for soundproofing to improve passenger comfort.

Narrow-body aircraft generally experience higher noise levels than wide-body aircraft due to shorter flight durations and less emphasis on soundproofing for passenger comfort. Noise levels range from 76dB(A) to 79dB(A) across different flight phases, with the loudest positions typically near the overwing exit. In comparison, wide-body aircraft exhibit lower noise levels, ranging from 68dB(A) to 74dB(A) [8].

Figure 2.1 illustrates the noise spectrum experienced by a passenger on a 787 airliner. It shows high noise levels between 100 and 1000 Hz, followed by a sharp decline. This peak overlaps with the frequency range of human speech, making it more noticeable and increasing discomfort and communication difficulty.

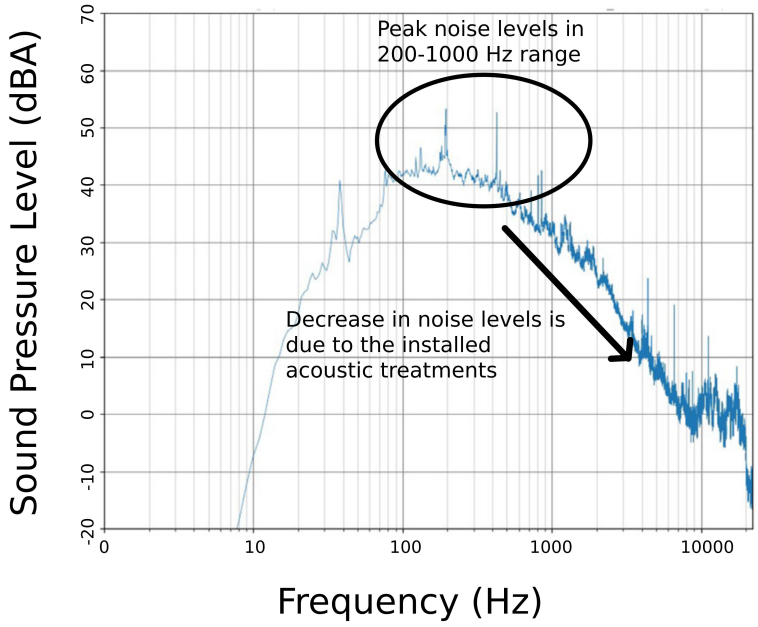

Figure 2.1: Cabin noise levels for a B787-900 aircraft [8]. The peak noise levels are observed in the 200-1000 Hz range. The downward slope of the noise levels is due to the installed acoustic treatments.

2.2. Current mitigation strategies

Currently, the primary approaches for noise mitigation consist of active and passive solutions. Active methods, like Active Structural Acoustic Control, utilise mechanical actuators to counter and suppress the vibrational response of the structure actively [9], similar to the noise cancellation feature on wireless headphones but placed on a wall instead on top of the ear. On the other hand, passive methods aim to enhance damping by employing materials with robust viscoelastic properties. These materials aid in reducing noise by absorbing and dissipating vibrations and sound energy. The two methods mentioned above exhibit efficiency in different regions of the sound spectrum, complementing each other. Active methods are particularly effective at mitigating low-frequency noise, while passive methods are better suited for attenuating higher-frequency noise. [10].

The active methods use dedicated transducers to turn the various cabin elements into sound-emitting surfaces. These solutions have significant drawbacks when implemented directly into the aircraft: they require constant power to operate, increasing the complexity of the wiring harness and interfering with maintenance, and require an extensive array of microphones to sample and compute the noise field continuously. Such solutions are most suitable for consumer products.

The passive method can be divided into reducing transmission and increasing sound absorption. While highly effective, reducing transmission necessitates structural modifications near the noise source. One common approach involves filling the space between the cabin sidewalls with multiple layers of porous materials such as foam or fibreglass. These materials act as barriers to prevent noise from entering the cabin [7]. Due to flanking, the sound-damping properties of the surrounding structure need to be enhanced. It is achieved through vibration isolation mounts or composite structures with better damping capabilities. There is also the option of using rubberised tapes if additional damping is required, but it comes at the cost of significantly increased mass [5].

The cabin's surface area should be enveloped with absorbent materials to minimise any open spaces that inadvertently become conduits for sound transmission, nullifying the intended acoustic treatment and instead functioning as a mere deadweight. The critical requirement for comprehensive coverage presents an intriguing prospect: transforming the cabin lining into a potent sound absorber. This integration harmonises the aesthetic appeal with soundproofing efficacy within a unified assembly, facilitating quicker maintenance access and offering a new path toward reducing overall weight.

2.3. State of the art

The following section provides an overview of the latest advancements in phononic metamaterial within academic research. The content is categorised based on the specific type of metamaterial discussed, such as acoustic black holes and Helmholtz-based metamaterials.

2.3.1. Film solutions

A recent advancement in phononic metamaterials involves a thin-film solution comprising an elastic membrane adorned with asymmetric rigid platelets. When impacted by sound, these membranes transform the energy from a pressure wave to mechanical deflection, achieving energy dissipation. The effect is lost if the membrane is installed too tight. These samples demonstrate remarkable absorption capabilities, particularly at frequencies where the sound wavelength in air is significantly larger than the membrane's thickness. The film structure consists of flexible substrates with rigid platelets attached. During resonance, the motion of these platelets creates a substantial concentration of elastic curvature energy at their perimeters. This unique mechanism minimally interacts with radiation modes, effectively converting acoustic energy into elastic energy within the membrane, resulting in high transmission loss [11].

Graphene, renowned for its exceptional in-plane stiffness and out-of-plane elasticity, presents new possibilities in phononic metamaterials. A highly effective acoustic absorber has been devised to enhance conventional acoustic foams by integrating graphene. This advancement entails a cellular arrangement of graphene aerogel drums, exhibiting robust resonances and remarkable dissipation efficiency across a broad frequency spectrum. A longstanding challenge in creating graphene-based absorbers has been overcome by combining graphene with traditional foams—namely, large-scale production and structural integrity. The resulting metamaterial showcases absorption coefficients of at least 0.8, commencing at 1000Hz and extending beyond 6000Hz for a thickness of 30mm [12].

2.3.2. Honeycomb membranes

Honeycombs are hollow cells, typically hexagonal, formed between vertical walls. These structures offer minimum weight and material cost. Researchers have successfully developed a lightweight phononic metamaterial with exceptional sound insulation properties featuring a hexagonal honeycomb-shaped frame covered by an elastic membrane [13], as depicted in Figure 2.2. Several studies have explored similar honeycomb-type acoustic metamaterials' sound transmission loss capabilities. One example is a constrained membrane-type phononic metamaterial, which achieved a peak sound transmission loss of 26 dB at 140 Hz. This metamaterial had a static areal density of 6.0 kg/m^2. Analysis of the vibration modes of the constrained membrane-type acoustic metamaterial revealed that the eigenmodes responsible for sound transmission loss dips shifted to higher frequencies, thereby significantly broadening its effective bandwidth [14, 15, 16].

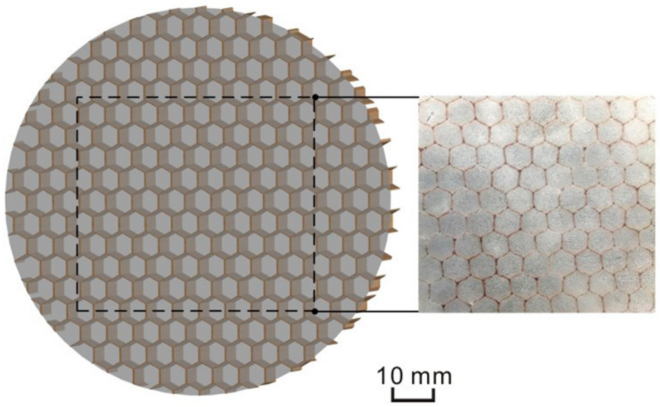

Figure 2.2: Honeycomb membrane-type acoustic material [13]. Absorption is achieved by transferring the incoming acoustic energy into the mechanical displacement within the membrane.

2.3.3. Acoustic black hole metamaterials

The emergence of acoustic black holes as metamaterials has revolutionised acoustic control possibilities in addition to membrane and thin-plate-type phononic metamaterials. Acoustic black holes are traps for flexural elastic waves based on structural heterogeneity, either in damping or stiffness. It involves integrating localised inhomogeneity within lattice structures. The change in mechanical properties interferes with wave propagation, reducing wave speed and enhancing absorption. Structures with embedded acoustic black holes exhibit reduced acoustic radiation and vibration levels.

Extensive studies have confirmed the efficacy of acoustic black holes in manipulating flexural waves, underscoring their significant potential for sound insulation applications. Researchers have utilised sound wave catheters or acoustic reverberation chambers to evaluate the sound insulation performance of 2D acoustic-black-hole plates. These assessments have unveiled that the influence of the damping layer on sound insulation predominantly occurs within the first-order resonance frequency and the damping

control region of the thin plate. Meanwhile, the modal damping loss factor exhibits improvement across the entire frequency range. However, it is worth noting that a thick damping layer can adversely impact sound insulation at specific frequencies. Applying a viscous damping layer to the surface of acoustic black holes reduces acoustic radiation efficiency [17, 18, 19, 20, 21].

2.3.4. Labyrintian metamaterials

Labyrinthian, or folding space metamaterials, are a family of phononic metamaterials that achieve the desired acoustic properties by arranging the transmission path in a maze-like geometry. The name comes from their similarity to a labyrinth. Absorption is achieved by leveraging the reflection and refraction of sound waves at each turn of the metamaterial.

Liang et al. [22] proposed the innovative ”folding space” method to achieve a high equivalent refractive index. This concept was further explored by studying the diffraction effects of periodically arranged spatially folded structures on the reflected sound field. They provided theoretical evidence for all-angle abnormal sound reflection. Additionally, it was demonstrated that when the incident angle surpasses the critical angle, the reflection gradient of acoustic metasurfaces can yield negative reflection.

Alongside the previously mentioned membrane or acoustic black hole metamaterials, labyrinth-type phononic metamaterials have garnered significant attention from researchers worldwide. An acoustic metamaterial was proposed, featuring labyrinth pipes arranged on one side of a main pipe. This configuration demonstrated remarkable sound insulation properties, particularly in the low-frequency range, and exhibited broadband effectiveness [23]. Building upon this concept, Liu et al. introduced novel acoustic metamaterials by employing a winding space to achieve broadband sound insulation [24]. By leveraging Fano resonance, they constructed an ultra-broadband sound barrier using space-coiling metamaterials. The sound transmission characteristics of these space-wound metamaterials under vertical incidence were described by a simplified model [25].

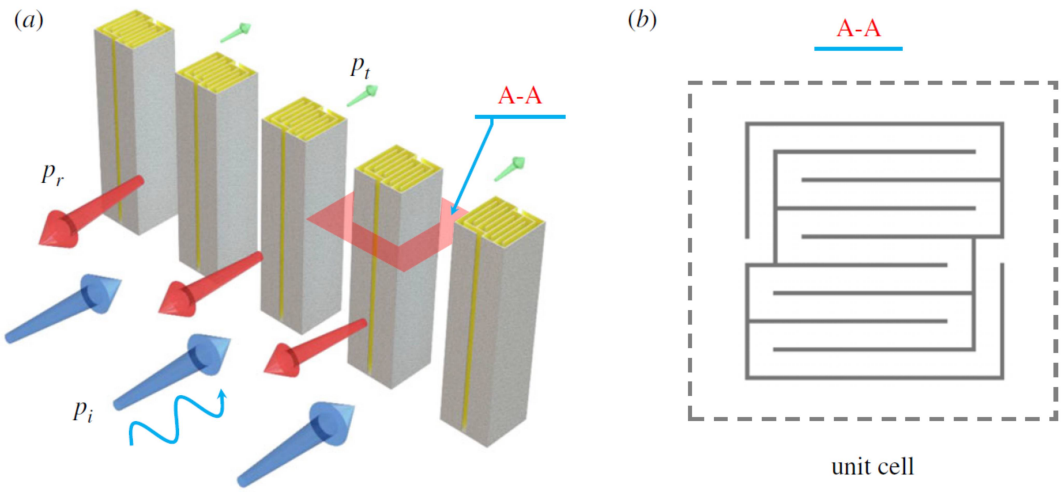

Figure 2.3: (a) Schematic illustration of the acoustic barrier assembled from Fano resonating elements. It efficiently blocks the incoming sound waves (pi) indicated by the blue arrows. The substantially reflected (pr) and heavily suppressed transmitted (pt) sound fields are indicated by red and green arrows, respectively. (b) Sectional view of the cross-section of a Fano unit cell [25].

2.3.5. Helmholtz resonator-based metamaterials

Perforated panels have been considered a next-generation acoustic treatment solution and have been successfully implemented as sound absorbers for aircraft engines. The traditional implementation of simply perforating a honeycomb panel is losing viability due to the shift towards a lower frequency spectrum found in newer powerplants. As presented in Figure 2.4, a newer patented solution uses large secondary cavities to achieve the desired absorption spectrum and performance [26].

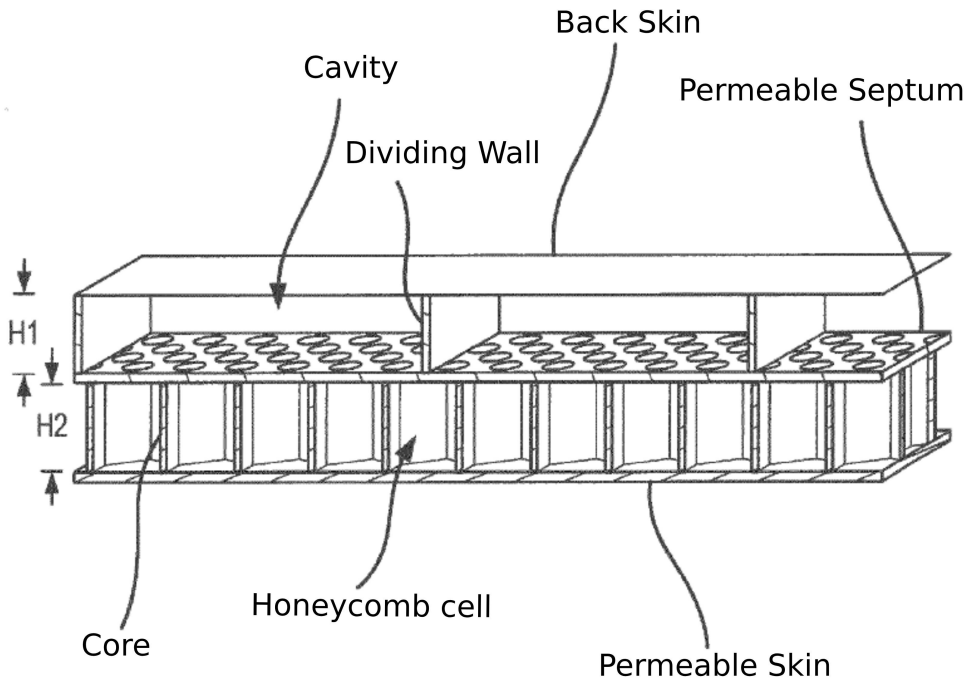

Figure 2.4: Acoustic panel comprising of large secondary cavities to attenuate low frequencies [26].

A perforated corrugated honeycomb composite structure was created by incorporating holes in both the top panel and the corrugated composite (Figure 2.5). This design aims to achieve exceptional sound absorption performance across a spectrum of frequencies [27]. Huang et al. [28] developed an acoustic system that combined a Helmholtz resonator with an embedded aperture. Experimental results demonstrated that this structure achieved flawless sound absorption even when its thickness was only 1/50 of the operating wavelength. The metamaterial is a superposition of conventional sandwich panel solutions and existing acoustic designs. The core combines a square grid intertwined with a corrugated wall. One of the face sheets is perforated in the centre of each grid square and continues through all corrugation walls. Doing so creates a series of resonating chambers of different volumes within each square grid cell.

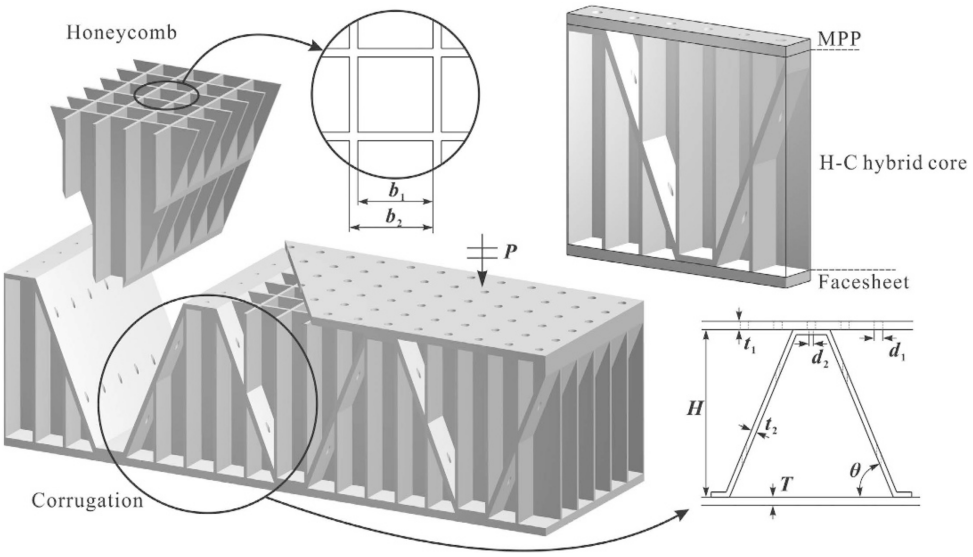

Figure 2.5: (a) Schematic of perforated honeycomb-corrugation hybrid (PHCH) metamaterial, which is composed of a micro-perforated panel as the top face sheet, a honeycomb-corrugation hybrid as the core and a panel as bottom face sheet. The corrugation is also perforated, just beneath the hole in the top face sheet, but can have different perforation sizes. (b) One periodic unit cell. The front and right honeycomb walls are cut off to see details inside. Sound absorption of the metamaterial is investigated for a plane acoustic wave normally incident on top factsheet [27].

Furthermore, a super surface was constructed by coupling two Helmholtz resonators with distinct resonance frequencies Figure 2.6 [29]. The authors proposed a particular frequency that falls between the resonance frequencies of the two Helmholtz resonators, where both resonators are simultaneously excited but with opposite phases. This unique configuration results in rapid decay of the sound wave in the direction of sound incidence, ultimately achieving perfect sound absorption.

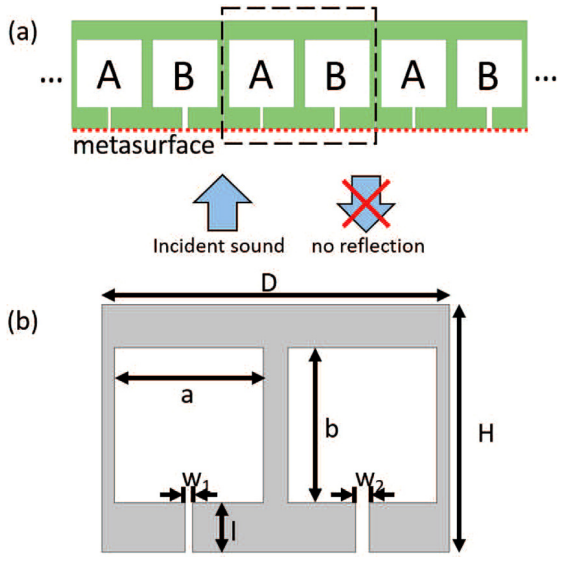

Figure 2.6: Helmholtz resonator metamaterial concept. Two resonators tuned at different frequencies achieve sound absorption at a target frequency where the individual acoustic elements are in opposite phases. Geometry and dimensions of the metasurface cell. (a) Schematic illustration of the metasurface and its unit cell, where A and B stand for different types of resonators; (b) Dimensions of the unit cell [29].

An alternative solution to address the challenge of achieving broadband low-frequency sound absorption involves coiled quarter-wavelength resonators. These resonators are designed in a spiral shape resembling a flat cylinder, allowing them to account for larger wavelengths effectively. The research by Carvalho [30] introduces a design and optimisation approach for fully parametric Archimedean spiral cavities. Through numerical simulations, the authors indicate that a configuration consisting of two spiral resonators connected in series can achieve two absorption peaks at the resonant frequencies of each device. Furthermore, the simulations reveal a minimum absorption coefficient of approximately 0.45 between the two resonating frequencies. Experimental results of the same setup confirm the devices' resonating frequencies and validate the system's maximum absorption coefficient. The experimental findings demonstrate a notable difference in the minimum absorption coefficient, with the lowest value close to 0.7.

The work of Catapane [31] investigates using archimedean spiral resonators (Figure 2.7) as the geometry of choice in sound-absorbing metamaterials. Resonators of different dimensions were assembled into various arrays (Figure 2.8), and their sound absorption capabilities were investigated using an acoustic test chamber under a diffuse acoustic field. Figure 2.9 shows the sound absorption spectrum of the samples used in the experiment. The paper does not explain the mechanism behind multiple absorption peaks. The expectation was for reduced absorption peaks to be visible at the octave (doubling of frequency) intervals instead of the tripling of frequency present in the publication.

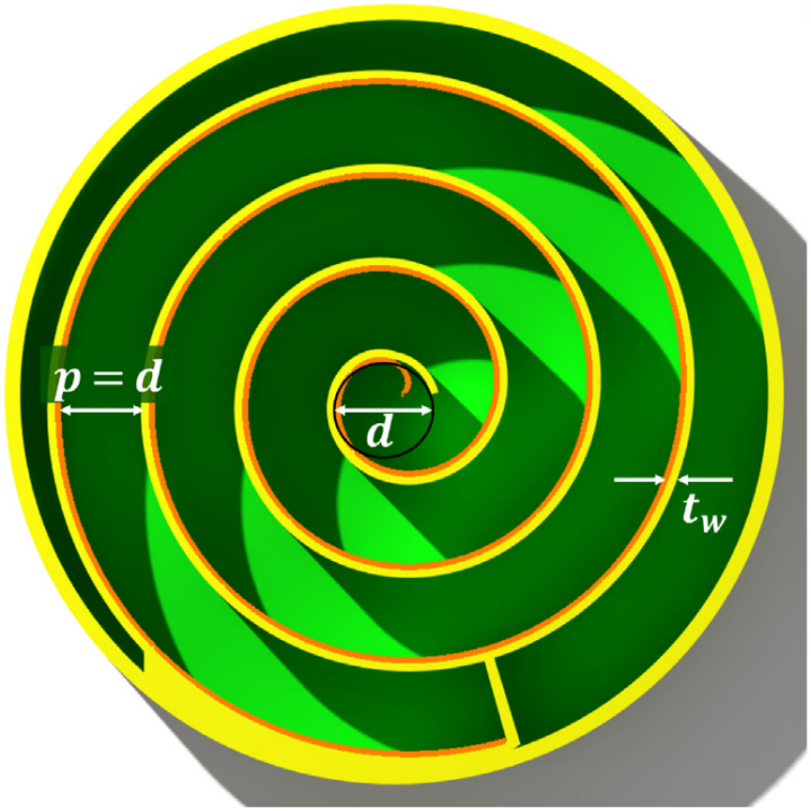

Figure 2.7: Front section of a spiral resonator without its top cover [31].

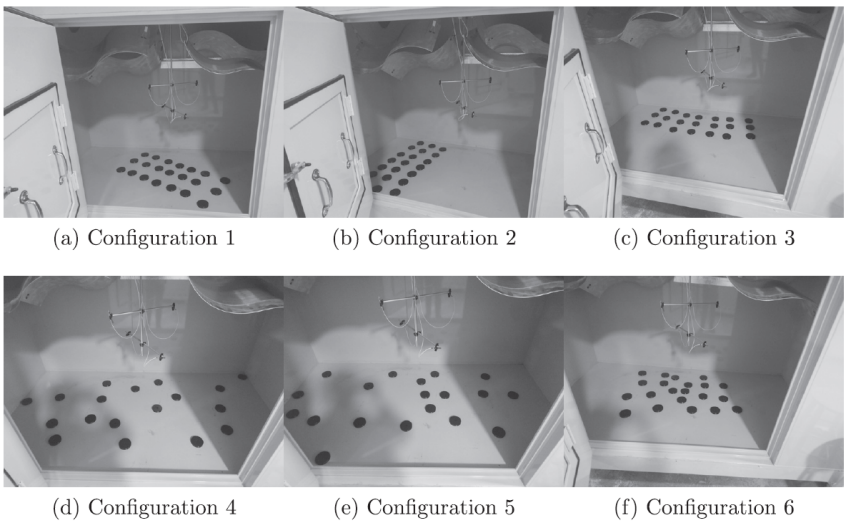

(a) Configuration 1 (b) Configuration 2 (c) Configuration 3

(d) Configuration 4 (e) Configuration 5 (f) Configuration 6

Figure 2.8: Pictures of the tested configurations [31]. a) orderly arrangement in the middle. b) orderly arrangement on one side. c) orderly arrangement along the back wall. d) random scatter. e) random scatter. f) grouped random scatter

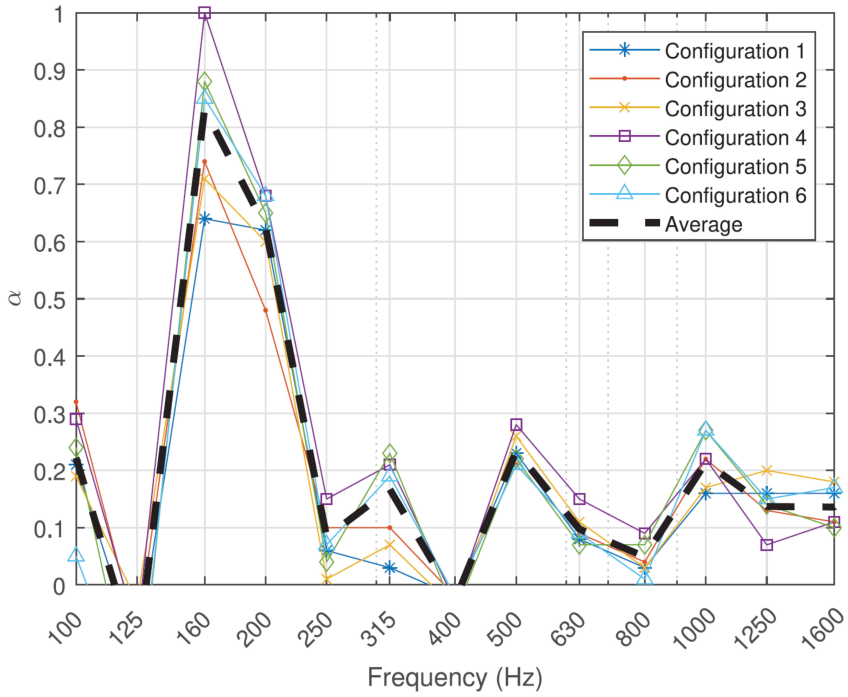

Figure 2.9: Sound absorption coefficient spectrum of various archimedean spiral configurations [31]. Peak absorption is achieved at the tuning frequency. A steep decay is observed, with no sound absorption at 35 Hz left and 90 Hz right of the resonance peak.

Fang et al. [32] investigated the sound absorption performance of a structure embedded with periodic partitions within a porous material. The objective was to enhance the sound absorption capabilities of the porous material. By manipulating the phase of the reflected waves, the researchers achieved a substantial increase in sound absorption compared to a uniform porous material. Furthermore, the sound absorption performance was enhanced even under oblique incidence.

Another study [33] explores the acoustic performance of double-degree-of-freedom Helmholtz resonators and multi-cell acoustic liners containing these resonators. Both experimental methods and finite element analysis are employed to investigate the system. The study focuses on varying the dimensions of the resonator's internal cavities to examine the impact of the volume ratio on acoustic performance. Figure 3.5 shows the experimental setup. The position of a septum controls the volume ratio between the two resonators.

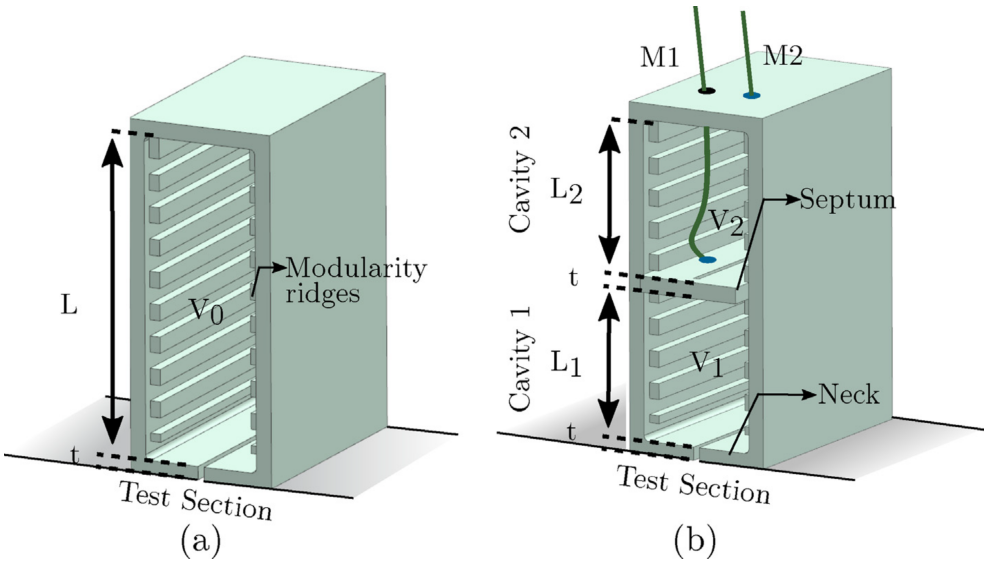

Figure 2.10: Experimental setup for testing the behaviour of multiple degrees of freedom resonators [33]. In this case, two resonators are attached in series. Sound waves enter through the neck of the bottom cavity and induce resonance within its volume. Part of the resonating air travels through a septum featuring an opening similar to the neck of the first cavity, inducing resonance in the top volume. V0 is the total volume of the structure. V1 and V2 are the volumes of the connected resonators. M1 and M2 are microphones associated with the volumes.

The transmission loss of periodic Helmholtz resonator-based metasurfaces (HRMS) has been investigated in depth by characterising the effect of each design parameter on noise reduction [34]. The metasurfaces increase both the performance regarding sound transmission loss and bandwidth. The peak improvement stems from the collective effect of the resonator cells within the array, amplifying the attenuation effect. The bandwidth expansion is due to cell arrangement, resulting in a diffuse or oblique sound field in the transmission zone.

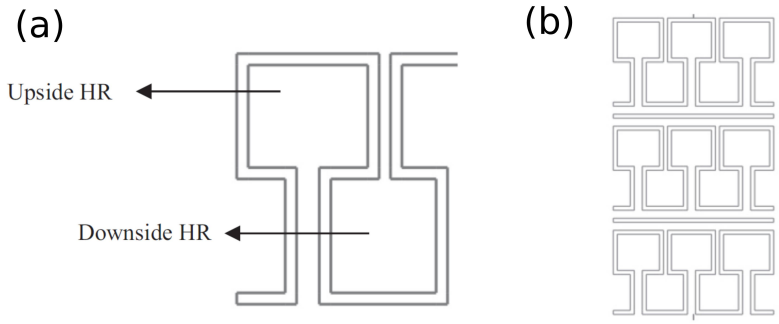

Figure 2.11: Ventilated Helmholtz resonators array [34]. (a) The principal unit cell of upside-down HRs. (b) Complete design of the metamaterial.

It was observed that by strategically placing lossy materials around the necks of single-resonance Helmholtz resonators, the absorption bandwidths could be expanded by as much as 100%. Three types of broadband acoustic absorbers were developed utilising this damped resonance effect: broadband absorbers (one-port), sparse broadband absorbers (two-port), and broadband duct absorbers (two-port). The approach to achieving broadband absorption allows for the creation of compact absorbers with a minimal number of resonances. It offers practical benefits by minimising the usage of porous materials, making it suitable for real-world applications [35].

Figure 2.12 illustrates the impact of incorporating a porous medium at the inlet of a resonator. An ideal Helmholtz resonator's bandwidth is at most 0.22 times the resonant frequency. By introducing lossy material over the opening, the bandwidth is doubled. Expanding the thickness of the porous medium to encompass the neck results in a bandwidth approaching that of F_{res}. While adding material inside the resonance offers diminishing returns, it still enables the creation of systems with bandwidths exceeding 100% of F_{res}, which helps create broader band absorbers.

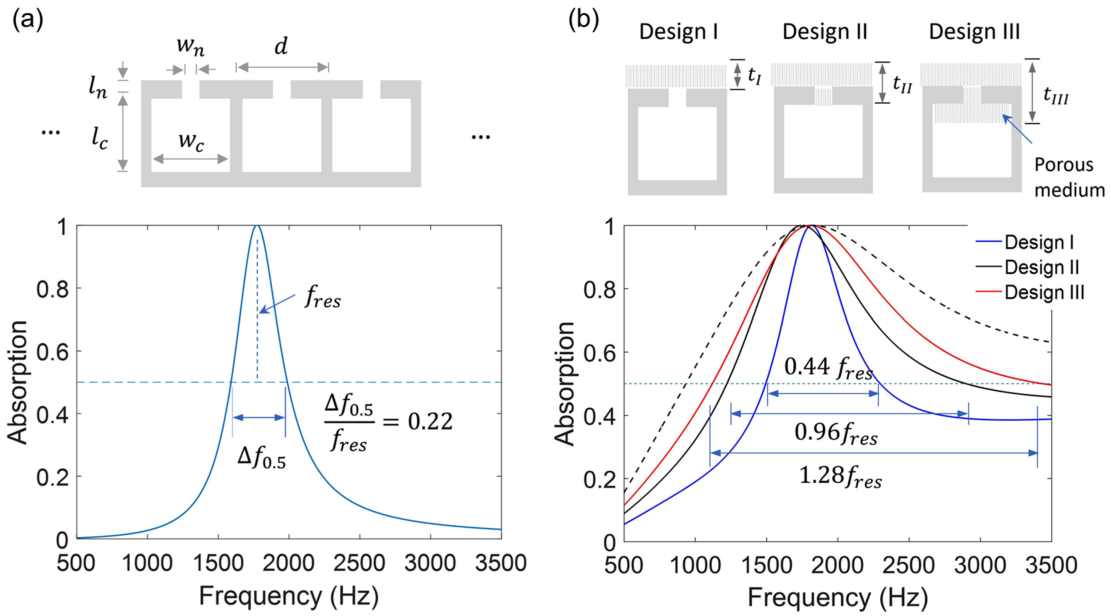

Figure 2.12: Effect of introducing lossy material at the inlet of a resonator array. (a) Array bandwidth without any porous medium. (b) Array bandwidth with porous medium on top [Design I], on top and in the neck [Design II], and porous medium on top, in the neck, and inside the resonating chamber [Design III] [35].

Figure 2.13 shows that it is possible to create nearly perfect broadband absorbers by stacking multiple HR arrays. The proposed design features a secondary, smaller resonator placed inside the main one's volume. The system's broadband aspect is reached by adding acoustic foam at the inlet of both resonators.

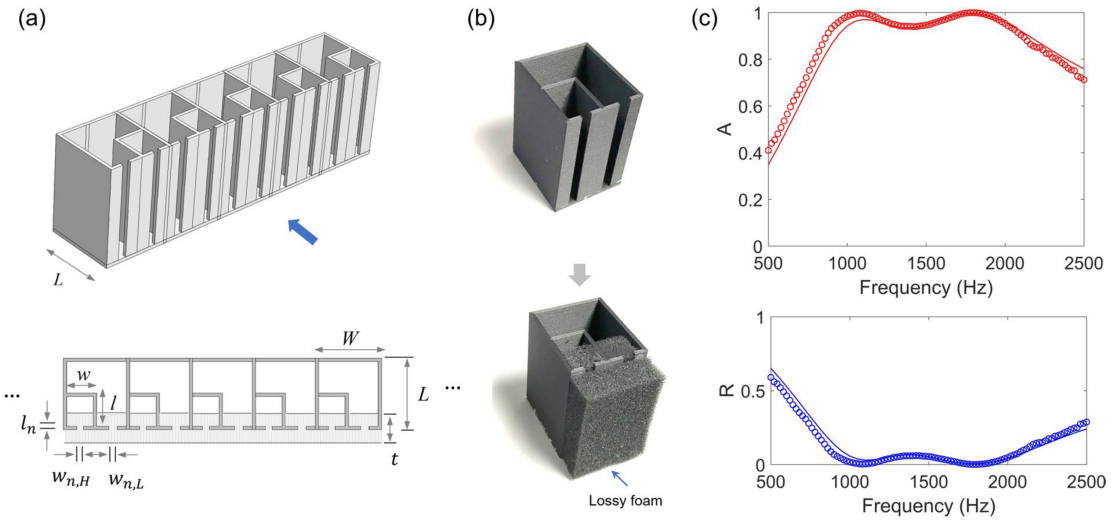

Figure 2.13: Example of a resonator array optimised for broadband absorption. (a) Geometry and lossy foam specification (W=40, L=43, w=18, l=20, $w_{n,H}$=4,$w_{n,L}$=5, t=foam thickness). (b) Printed specimen without (top) and with(bottom) lossy foam. (c) Top: Absorption spectrum of the sample, with lossy foam. Bottom: Reflection spectrum of the sample, with lossy foam [35].

2.4. Research gap

Recent research in metamaterials has primarily focused on evaluating the performance of the individual unit cell, resulting in a disparity between laboratory observations and real-world applications. The effectiveness of implementing resonators is contingent upon the characteristics of the target structure. For instance, if the structure possesses robust intrinsic sound absorption capabilities, the influence of the resonators is minimal. Conversely, a structure that exhibits excessive acoustical transparency is unsuitable for integrating metamaterials, as it allows resonating sound waves to pass through. Furthermore, critical factors such as manufacturability and weight have been overlooked. The literature review has identified the following gaps in the current understanding of resonant phononic metamaterials:

Integration and performance in lightweight structures: Limited research exists regarding the effective integration of Helmholtz resonators into lightweight composite sandwich panels comparable to those utilised in aircraft. Most studies concentrate solely on the acoustic properties of Helmholtz resonators, disregarding their implications for the panel's strength, stiffness, and overall performance.

Manufacturing processes and practical applications: Existing studies provide inadequate insight into the manufacturing processes of Helmholtz resonator-based metamaterials. These materials are typically fabricated using sophisticated 3D printing or laser cutting techniques. Moreover, there is a shortage of investigation regarding the practicality and scalability of integrating these materials into mass-produced structures.

Acoustic and mechanical balance: Insufficient attention has been directed towards striking a balance between the acoustic advantages of Helmholtz resonators and mechanical properties, such as strength and weight. Many studies neglect to address how the integration of these resonators impacts overall weight and mechanical performance.

2.5. Research objective

The research aims to establish how a traditional honeycomb core can be acoustically enhanced using Helmholtz resonators. In achieving this goal, the research gaps regarding the integration and performance of metamaterials in lightweight structures and the relationship between mechanical and acoustic balance will be addressed. As highlighted in magenta in Figure 2.14, the cabin lining is enhanced by integrating Helmholtz resonators within its structure.

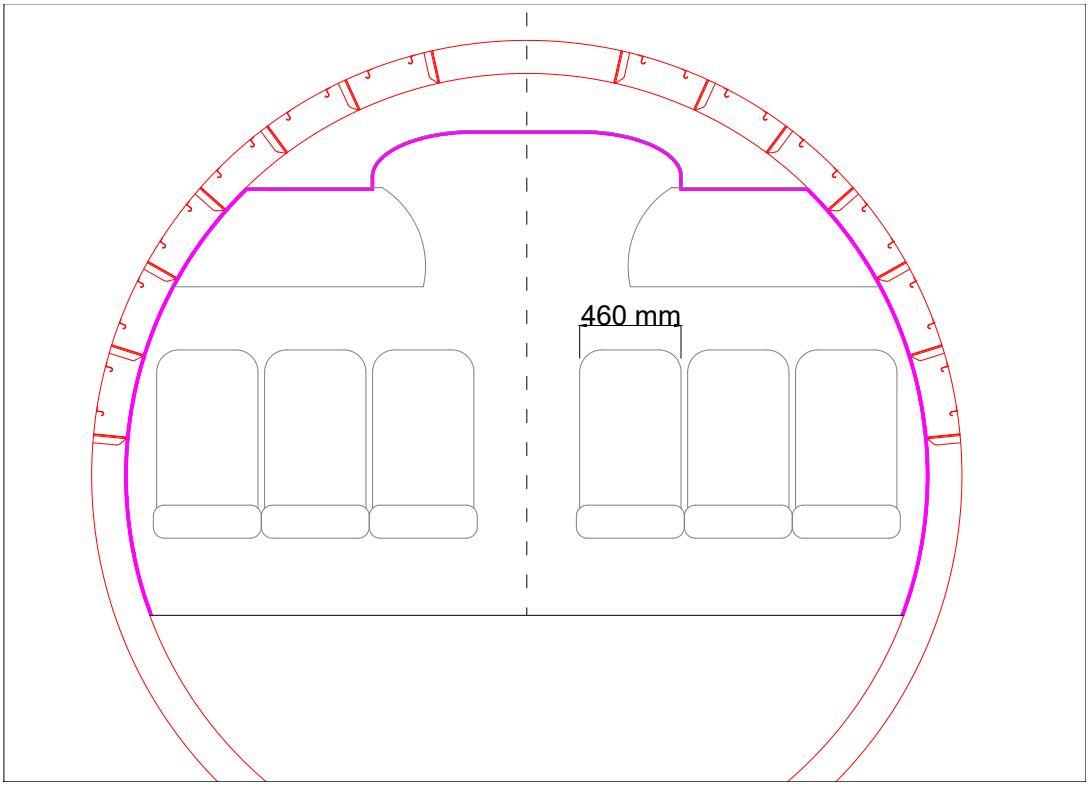

Figure 2.14: Cabin elements most suitable for enhanced sound absorption capability is depicted in magenta, namely the lining, ceiling panels, and the top and back walls of the luggage bins. Artistic representation of a narrow-body aircraft, such as an A320.

Figure 2.15 further details the metamaterial integration. The lining is comprised of honeycomb composite sandwich panels. The Helmholtz resonators are placed entirely within the volume of the honeycomb cells, with the inlets facing away from the passengers. This placement is chosen due to the stakeholder requirements of the passengers, panel manufacturers, and maintenance crews. The passengers desire a safe and comfortable flight. Placing the inlets towards the cabin interior creates insecurity, negatively impacting the passenger's sense of safety. Doing so also exposes the metamaterial to bad actors who, for example, might dispose of their chewing gum in one of the resonator inlets. The panel manufacturers and maintenance crews require a panel that is easy to handle, transport and store. Placing the inlets within the resonator chamber allows for a thin panel with two flat sides and protects the inlets from damage. Handling and storing the panels becomes no different from any other sandwich panel.

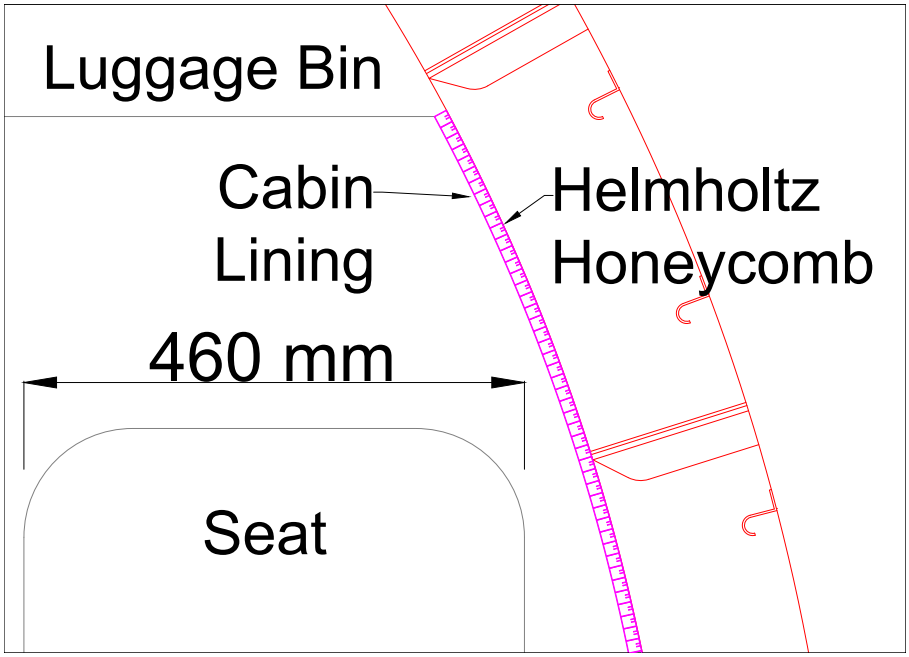

Figure 2.15: Detailed drawing of Helmholtz resonators integration into the cabin lining. The resonator inlets face away from the passengers. The acoustic panel exhibits two flat faces, with the resonator inlets placed inside the resonance chamber.

2.6. Research question

The first step in determining the practicality of integrating Helmholtz resonators into thin, lightweight acoustic panels is to establish which requirements must be imposed during the metamaterial design phase. This exploratory study addresses various aspects of this integration, from acoustic performance to material reinforcement and weight implications. The research question is formulated as follows:

Main research question

What design requirements shall be defined to create Helmholtz resonator-based metamaterials used as core materials in lightweight composite sandwich structures with applications in aircraft cabin elements?

Supporting subquestions:

- **How does the relationship between acoustic performance and structural design affect the absorption capability of thin-walled metamaterial structures, and what design strategies can enhance this performance?** Investigate the relationship between acoustic performance and structural design. This investigation aims to determine the impact of thin-walled structures on the absorption capability of the metamaterial and establish what design strategies can be used to allow for lightweight metamaterials with high acoustic performance.
- **How does placing the resonator inlet within the resonance chamber affect the creation of flat resonator arrays with maximised resonance volumes for a given thickness?**
- **Which resonator array topologies are most suitable based on the findings of previous investigations?**
- **How does the implementation of resonators affect the failure modes of composite honeycomb sandwich panels, and what mitigation techniques can be employed without compromising acoustic performance?** The goal is to determine the failure modes most affected by the presence of the resonators and provide mitigation techniques which do not compromise the acoustic performance.

- **What are the appropriate reinforcement materials for composite skins?** Three different fibre types will be tested: fibreglass, a common reinforcement fibre used in the cabin; carbon fibre, due to its high specific stiffness; and flax fibre, a natural alternative which boasts superior damping properties.
- **What are the weight implications of integrating Helmholtz resonators into composite honeycomb sandwich panels?** Answering this question is critical, as reducing the weight of aircraft components impacts the environment and operational costs.

The following flowchart illustrates the research process and stages involved in addressing the research questions:

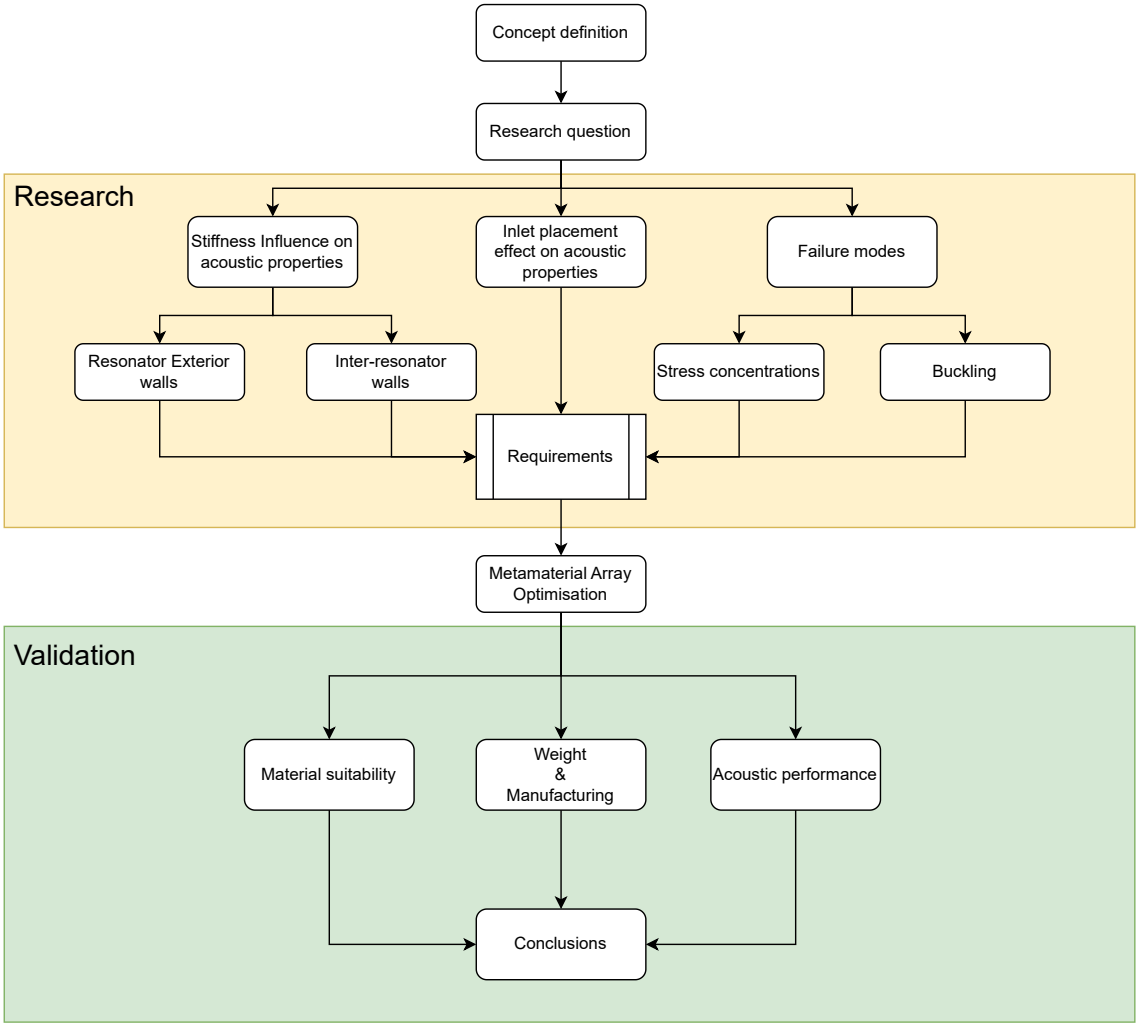

Figure 2.16: Reserch flowchart

3

Methods

The following chapter describes the methodologies for manufacturing test samples and acoustic panel prototypes and the approach to acoustic testing. First, the specific production methods and tools for creating test samples and acoustic panel prototypes are outlined. Next, an overview of the acoustic testing approach is provided, offering insights into the equipment, test setup, and rationale behind the chosen methodology.

3.1. Manufacturing methods

3.1.1. Fused Filament Fabrication

Fused Filament Fabrication (FFF) was selected as the manufacturing method for this project. This technique was employed to create samples for the resonator exploration phase of the design process and to construct the honeycomb core of the metamaterial sandwich panels. As an additive manufacturing process, FFF builds the desired part layer by layer. The method utilises a continuous thermoplastic polymer filament as the base material, fed through a moving extruder head and deposited onto the growing workpiece.

The generation of the machine toolpath involves analysing the part's geometry using a dedicated software package known as a slicer. The slicer divides the part into evenly spaced layers of the desired height. It then analyses each slice to identify the contours of the section. Finally, the program generates the necessary machine commands based on the user's specifications.

3.1.2. Printer and setup

The machine used in this project is a BambuLab X1-C equipped with a 0.5 mm nozzle and the standard Bambu Cool Plate. The filament material is eSun PLA+. The printer is set up according to the material manufacturer's recommendations. Before each print, the print bed is cleaned with 70% ethanol, and a layer of 3DLAC adhesive spray is applied to ensure bed adhesion. The flow rate and bed levelling calibrations were repeated at the start of each print to account for environmental temperature variations and water content within the filament.

3.1.3. Printed sample manufacturing

The samples' print orientation was chosen to achieve the shortest manufacturing time. The extruded resonator samples were printed upright, with the openings perpendicular to the print bed. It results in the fastest prints, minimising the bridging required to create the top of the surface. Consequently, the perimeter walls define the minimum wall thickness: 0.5 mm. The array samples are best manufactured with the openings facing the print bed. This orientation ensures consistent manufacturing. In other orientations, such as the one used for the extruded samples, most tool paths feature an overhang or outright bridging, increasing the number of failure points in the manufacturing process.

3.1.4. Composite manufacturing: vacuum infusion

The composite elements of the samples are manufactured using vacuum infusion. The process relies on pressure difference to transfer the resin matrix into the reinforcement fibre. The reinforcement fibre is placed in the desired lay-up onto an aluminium plate treated with a release agent. A nylon cloth, known as peel ply, is applied on top of the reinforcement to imprint a rough texture onto one side of the laminate. The rough texture facilitates bonding during the sandwich panel's manufacturing. A perforated film of high-density polyethene is laid on the peel ply. Next, a flow media is placed on top. The flow media facilitate the resin flow along the composite part, allowing for infusion through the thickness, which ensures a higher quality infusion. Finally, the vacuum lines are placed, and the stacking is sealed using a nylon-based bagging film. The bagging film is attached to the build plate using a rubberised sealant tape. A list of all the ancillary materials can be seen in Table 3.1.

Material	Function
Al plate	Ensure a flat surface.
Release agent	Prevent the part from sticking to the build plate.
Peel ply	Imprint rough texture to facilitate secondary bonding.
Release Film	Facilitate release of flow mesh from rest of stacking.
Flow Mesh	Facilitate the resin flow across the surface of the laminate.
Bagging film	Create a sealed enclosure, and apply pressure for consolidation.

Table 3.1: List of ancillary materials used in the vacuum infusion process and their function.

Three different fibre types are used for the composites: fibreglass, carbon fibre, and flax fibre. The specification of the manufactured composites is presented in Table 3.2. For the samples where the fibre is in the form of a woven fabric, a lay-up of [0/0]t was used. For the uni-directional (UD) fibre, the mechanical properties of a woven fabric were approximated by rotating one of the plies by 90°. The composite laminate thickness was measured after consolidation.

Fabric type	Weave	Specification	Lay-up	Thickness (mm)
Fibreglass	8HS	E-Glass	[0/0]t	0.5
Carbon fibre	2x2 Twill	AS4	[0/0]t	0.5
Flax	UD	Natural fibre	[0/90]t	1.5

Table 3.2: Composite face sheet material and lay-up specification.

3.1.5. Acoustic sandwich panel fabrication

Manufacturing the acoustic sandwich panels utilises a secondary bonding process involving the adhesion of face sheets to the core. A waterjet cutter was employed to fabricate the face sheets. The presence of the resonator openings necessitated the use of the water jet. Two large and four small face sheets were prepared for the fibreglass and carbon-reinforced laminates. Figure 3.1 illustrates the nesting used to generate the waterjet tool path.

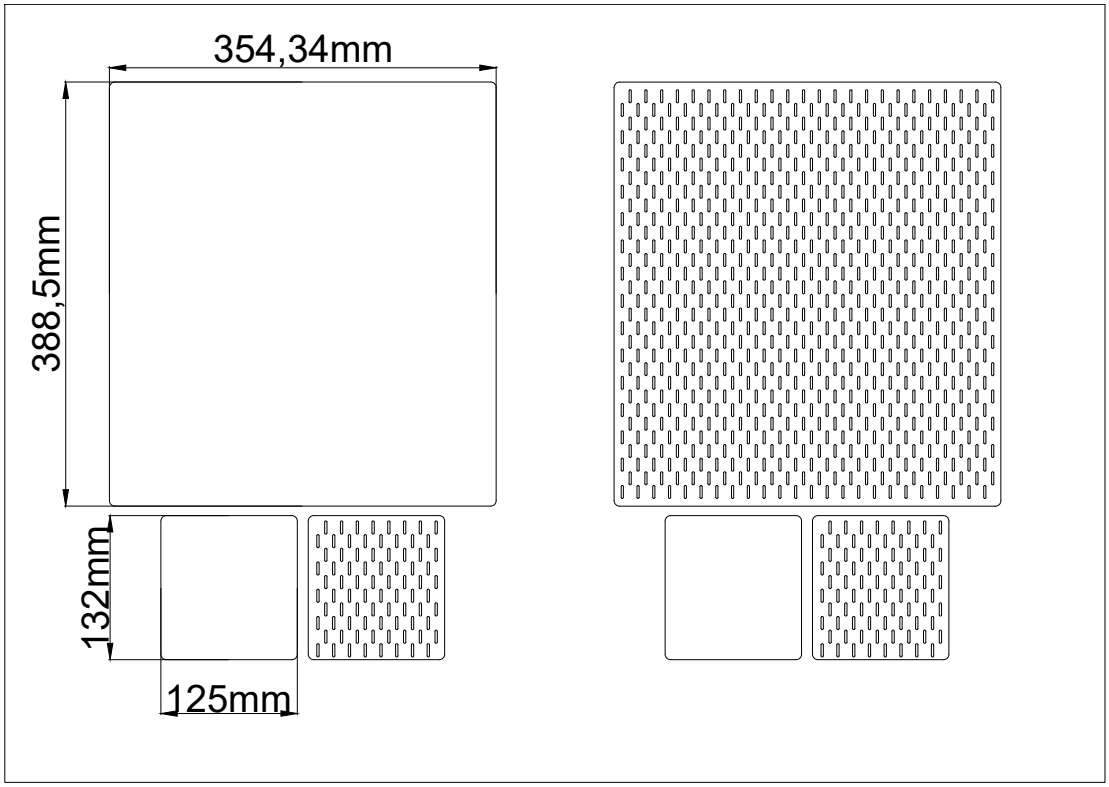

Figure 3.1: Nesting drawings used to cut the face sheets on the waterjet machine.

Additional tooling was developed to ensure the openings remained unobstructed during the bonding process. The jig, which consists of a flat plate adorned with raised pins, matches the geometry of the perforated face openings, as depicted in Figure 3.2. The perforated face sheets are placed onto the jig and generously slathered in Araldite AW106 adhesive, as seen in Figure 3.4. Before attachment to the metamaterial core, the face sheets were removed from the jig and inspected for obstructions. During the curing process, the panels were positioned with openings to prevent the adhesive from pooling into the perforations. The adhesive curing process was accelerated at 40°C for three hours.

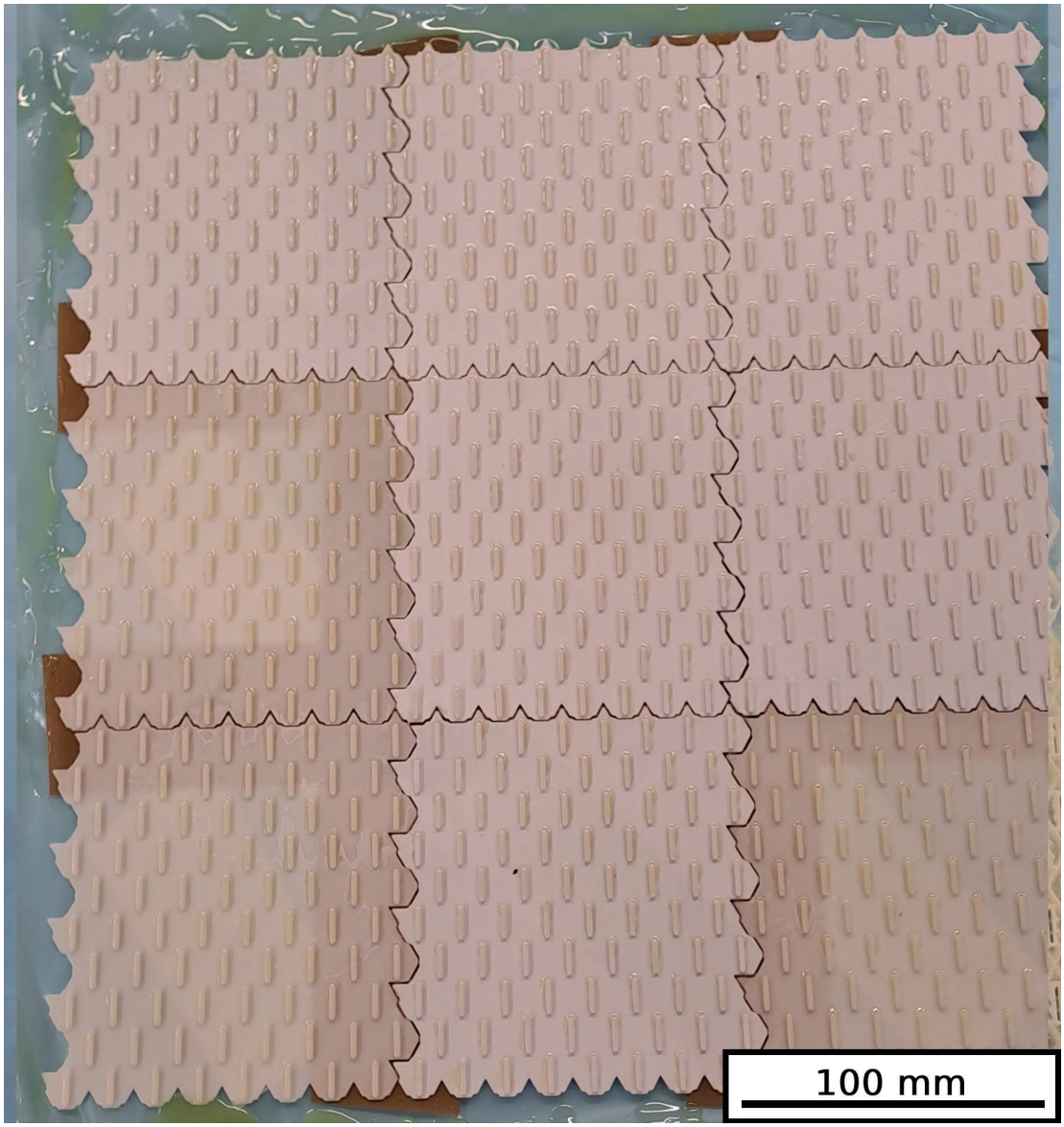

Figure 3.2: Jig used for the application of the adhesive. The raised pins match the geometry of the slots in the perforated face sheet. The height of the pins is the same as the thickness of the perforated sheet.

Figure 3.3: Perforated carbon fibre face sheet placed on the jig. The adhesive is applied as if the component was not perforated. Upon removal, the holes remain unobstructed.

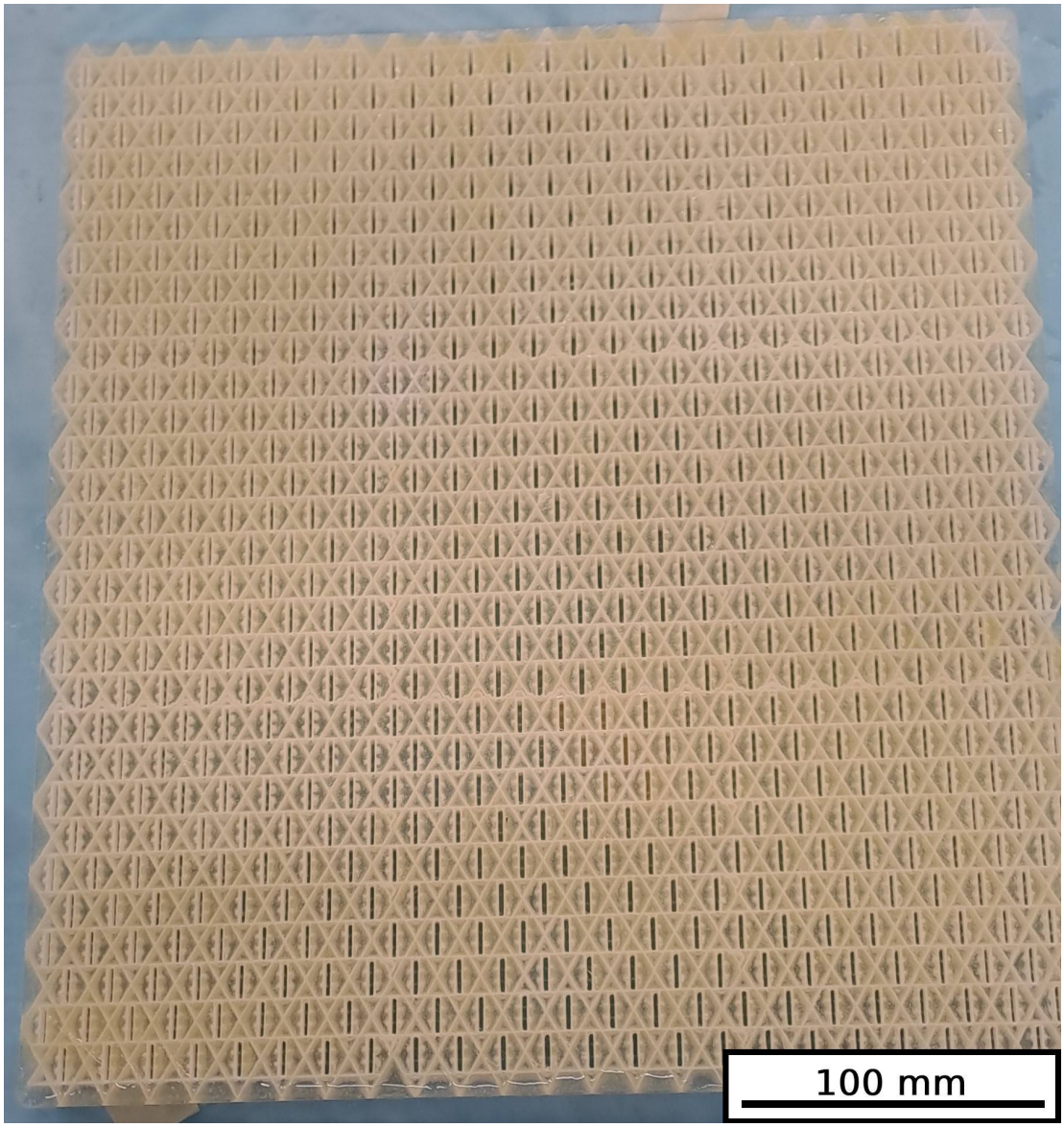

Figure 3.4: Fibreglass phononic metamaterial panel before consolidation. The panel is placed with the openings on top to ensure they remain unobstructed during the adhesive's curing cycle.

3.2. Acoustic test methods

The acoustic testing methodology aims to replicate the conditions encountered in an aircraft, where noise travels from the aircraft's skin inwards towards the passengers through the lining. This approach directly relates the performance of the metamaterial to a passenger's experience. The sound levels are measured after passing through the metamaterial. This testing method was used in each project phase to guide the research process and validate the implemented design solutions. Throughout the project, the purpose of the acoustic tests varies from observing acoustic absorption generated by the resonators to validating the final design by measuring its performance. The following equipment was used for the experiment:

- Digital audio editor for playback and spectrum analysis
- Bluetooth speaker
- Soundproof box
- SPL meter
- Quiet room

The purpose-built soundproof box for this project consists of fibre-reinforced drywall with walls measuring 25 mm thick. The interior is lined with commercial soundproofing foam. The lid is adhered to the rest of the enclosure and features an aperture for the samples. The enclosure measures 425mm tall. The base is square and has 270 mm sides. The microphone is held 150 mm from the sample during acoustic testing. The 150 mm dimension estimates the distance between a passenger's head and cabin lining when seated near the window. Figure 3.5 provides a schematic of the test setup.

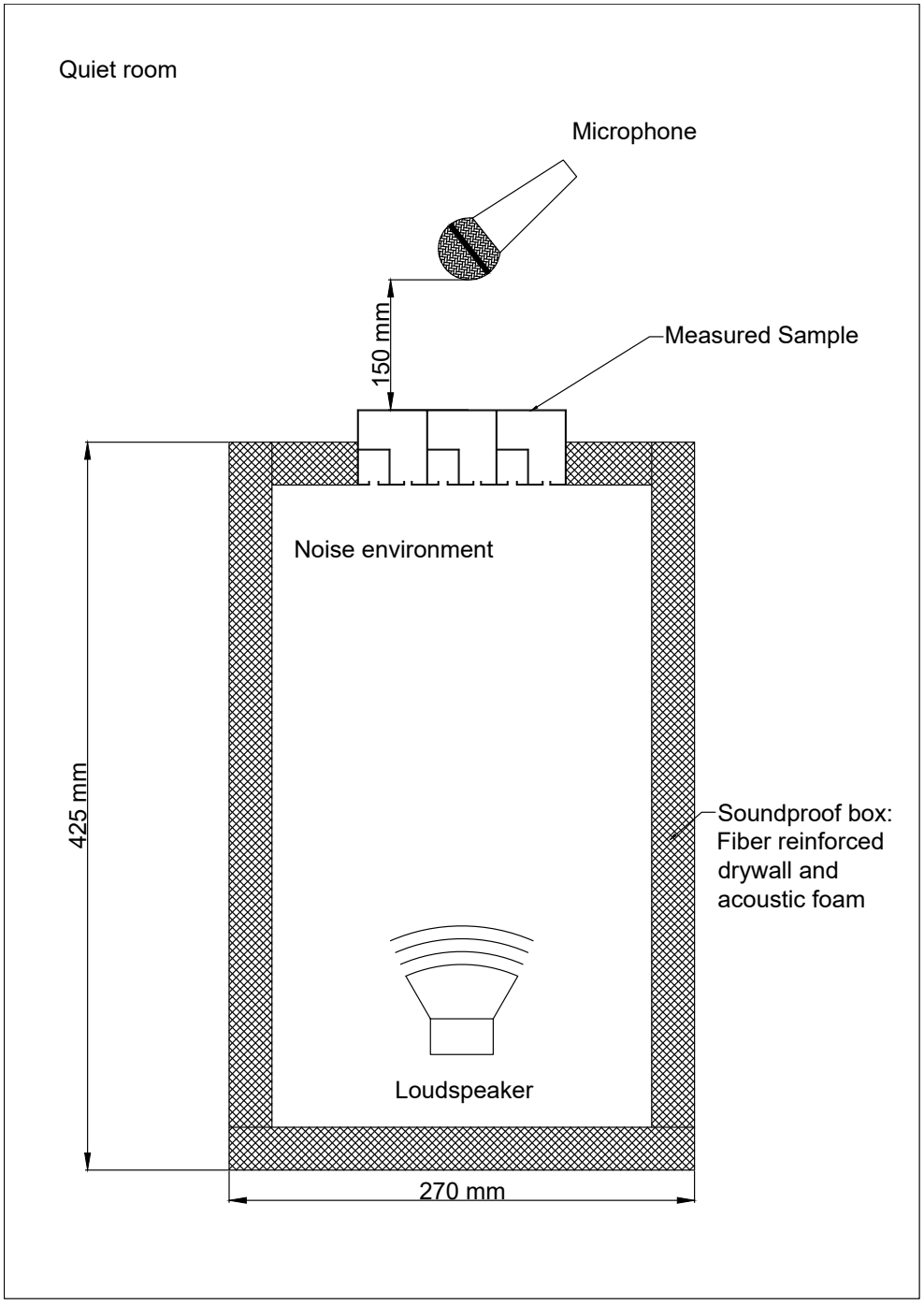

Figure 3.5: Experimental setup. A speaker is placed inside a soundproof box. Sound absorption is measured as the difference in sound pressure levels between open and closed box conditions. The test sample is used as the lid. The speaker volume is calibrated so there is no leakage through the box walls.

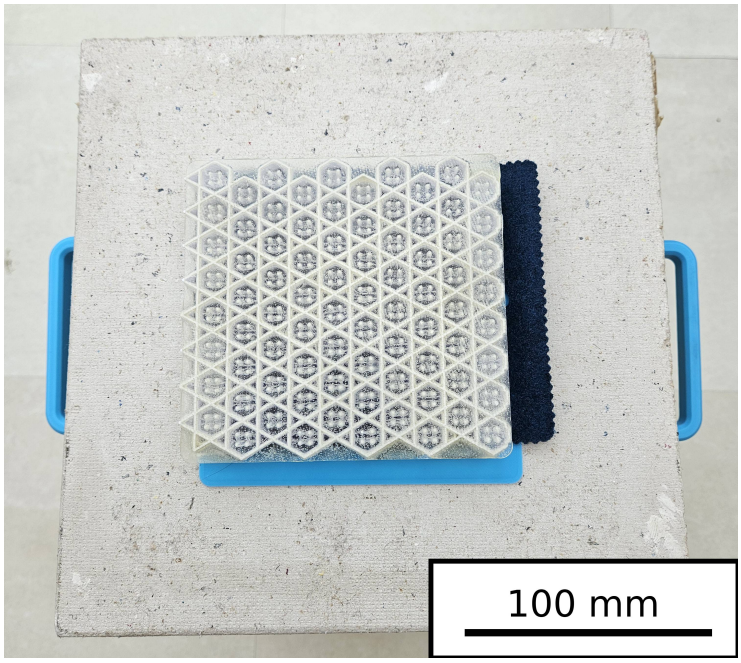

Figure 3.6: Photo of the experimental setup with the sample in place, top view. The sample is placed with the resonator inlets towards the noise source.

3.2.1. Experimental setup and calibration

White noise is limited to the 500-5000 Hz range for the acoustic tests, corresponding to the Speech Interference Level spectrum, and is played through the speaker. The speaker volume is calibrated to ensure no sound transmission occurs through the walls of the soundproof box. Calibration involves closing the enclosure using a lid made of the same material as the soundproof box and gradually increasing the volume until the sound can pass through the enclosure. The desired volume level is slightly below the threshold at which noise starts bleeding through. Following calibration, the acoustic tests were performed.

3.2.2. Baseline measurements

The first step in each test was establishing baseline values for the maximum and minimum possible noise levels. The initial baseline was obtained with the soundproof box open, with no sample or lid, to determine the acoustic power released by the speaker and its performance at various frequencies. The second baseline measured the minimum noise level with the speaker turned off, providing the noise floor of the setup.

3.2.3. Acoustic sample measurements

The process of measuring the acoustic performance of each sample is simple: the sample is inserted into the opening of the soundproof box, acting like a plug. The sound pressure level (SPL) passing through is then measured, and a 30-second recording is saved. The recording and SPL measurement provide sufficient information to recreate the spectrum of the noise passing through the sample.

3.2.4. Data analysis

Audacity, an open-source digital audio editor capable of noise generation and spectrum analysis, was used to analyse the recordings. The software generated the noise spectrum, which was correlated with the SPL measurement to obtain a breakdown of the sound pressure level at each frequency. This process was repeated for all measurements, including the baselines.

The analysis involves determining the SPL difference between the samples and the first baseline, comparing the SPL difference between the metamaterial and a sample without resonators, and computing the absorption coefficient. The first analysis shows how much each sample reduces the noise levels. The second analysis is focused on identifying the effect of the resonators. If the sample with resonators performed worse than one without, it would indicate that either the resonator is improperly designed or the concept is flawed. The final analysis aims to normalise the absorbed noise power. The absorption coefficient is the ratio between the sound power emitted by the speaker and the sound power absorbed by the samples. Normalisation converts the SPL from a logarithmic to a linear scale, providing a different point of view to the noise absorption potential of the samples.

4

Results and discussions

This chapter presents the research findings, beginning with a detailed account of the design process. It focuses on the stakeholders affected by the acoustic panel and the various investigations conducted. Each investigation is presented in a standalone section encompassing methodology, results, and discussion, concluding with the identified requirements.

This presentation method is chosen due to the exploratory nature of the research, where the design process serves as a research focus and a methodological approach. The investigations are strongly linked, with the results from one phase being implemented in subsequent phases for validation. This iterative approach ensures thorough validation and refinement of the acoustic panel design, culminating in a comprehensive evaluation of its performance and feasibility.

Following the detailed design process, the chapter proceeds to the final design. This section includes an evaluation of the design outcomes, validated for acoustic performance, the face sheet material suitability study and an analysis of its weight and manufacturability. The chapter provides a holistic view of the design process, from understanding stakeholder needs to finalising a manufacturable and effective acoustic panel. This approach demonstrates the research findings and establishes a solid foundation for future work in acoustic panel design.

4.1. Design process

This section details the design process of the metamaterial core, from identifying the stakeholders and their needs to designing the resonators and performing the necessary investigations to answer the research question. The stakeholder needs are the driving force behind the presented research. The design process is documented to highlight the methodology, results, and discussions, concluding with the key requirements.

4.1.1. Stakeholder needs

The first step is identifying the stakeholders, including all parties interacting with the component at individual and organisational levels. The stakeholders are grouped into the following categories:

- Passengers: These are the airline and aircraft customers. They desire comfort and safety when flying, and the aircraft's appearance easily influences their perception of safety. Images of temporary repairs, like speed tape on aircraft structures, often raise safety concerns. Similarly, the cabin's appearance is crucial; dirty or misaligned panels can increase flight anxiety. For this reason, the resonator inlets must be hidden, as visible inlets can make panels appear weak and flimsy.
- Maintenance Crews: This category includes all personnel responsible for maintaining the aircraft's safety, from engineers to technicians. Factors such as ease of installation and accessibility significantly impact their performance. The panel design must facilitate easy handling, storage, and transportation.

- Aircraft Operators: Their primary goal is profitability, which involves reducing operational costs and attracting customers. The panel's weight affects fuel consumption and emissions, impacting costs and environmental image. Additionally, operators aim to enhance passenger comfort through improved architectural design and noise reduction.
- Manufacturers: This group focuses on the panel's manufacturability. Given the current phase of metamaterial integration, satisfying manufacturing needs is challenging. The design requires extensive knowledge of various manufacturing processes to ensure feasible mass production. Collaboration between designers and manufacturers is crucial.

The proposed acoustic panel concept addresses all stakeholder needs. The resonator inlets are strategically placed to avoid imparting a feeling of flimsiness and to provide a clean workspace for cabin architects. The panels are designed flat, with the resonator inlet placed within the resonance chamber to improve handling, storage, and transportation. The design prioritises weight minimisation while ensuring enhanced soundproofing through the resonators. Finally, the panels are designed to be manufacturable.

4.1.2. Resonator design

The approach to resonator design is centred strictly on the resonance frequency, opting to neglect the more complex phenomena leading to sound absorption. This approach is chosen because the research focuses on integrating acoustic devices in lightweight structures. Once suitable structural design processes and requirements are identified, the resonators can be optimised for maximum absorbance.

The Helmholtz resonators are simple acoustic structures with enclosed volumes communicating to the outside environment through a necked inlet. Objects with structures identical to the Helmholtz resonator are common in daily life: empty water bottles. The resonance frequency depends on the enclosed volume, inlet opening and inlet length. The formula for determining the resonance frequency is presented in Equation 4.1. c is the speed of sound, A_0 is the inlet opening area, V is the resonant volume and L_0 is the inlet length. Two-dimensional resonators are also possible. They consist of an extruded cross-section, capped at both ends to create a fixed volume. The advantage of this simplification is the ease of manufacturing. Two-dimensional resonator samples can be produced much more quickly than their 3D counterparts. The formula for resonance frequency can be easily derived. The opening area is dependent on the opening size and resonator depth. The resonant volume depends on its height, width and depth. Since the depth is present in the numerator and denominator, its contribution cancels out, leading to Equation 4.2. O is the opening size and A is the resonant chamber cross-sectional area.

$$F_{res} = \frac{c}{2\pi}\sqrt{\frac{A_0}{V \cdot L_0}} \tag{4.1}$$

$$F_{res} = \frac{c}{2\pi}\sqrt{\frac{O}{A \cdot L_0}} \tag{4.2}$$

4.1.3. Influence of cell stiffness on acoustic damping

The investigation into structural stiffness's influence on Helmholtz resonators' acoustic properties is split into two phases. The outer wall's stiffness effect is determined in the first phase. The design proposed by Lee [35] is manufactured with the minimum wall thickness allowed by the manufacturing setup: 0.5 mm, or one wall line. The sample is tested according to the previously presented method for acoustic testing. The design is deemed sufficiently stiff if sound absorption is observed at the resonance frequency. If absorption is not observed, the number of wall lines increases until absorption is observed. The resulting outer wall thickness is then correlated with a characterised composite material to establish the minimum amount of plies needed to maintain acoustic performance. The investigation's second phase focuses on the resonator's interior walls, which function as barriers between neighbouring resonators—insufficient stiffness results in the resonators influencing each other, compromising acoustic performance and complicating the tuning process. Two solutions are investigated: increasing the wall thickness and introducing non-resonant elements. The findings of this investigation are used to define metamaterial design requirements. A flowchart of the work performed during this investigation is presented in Figure 4.1.

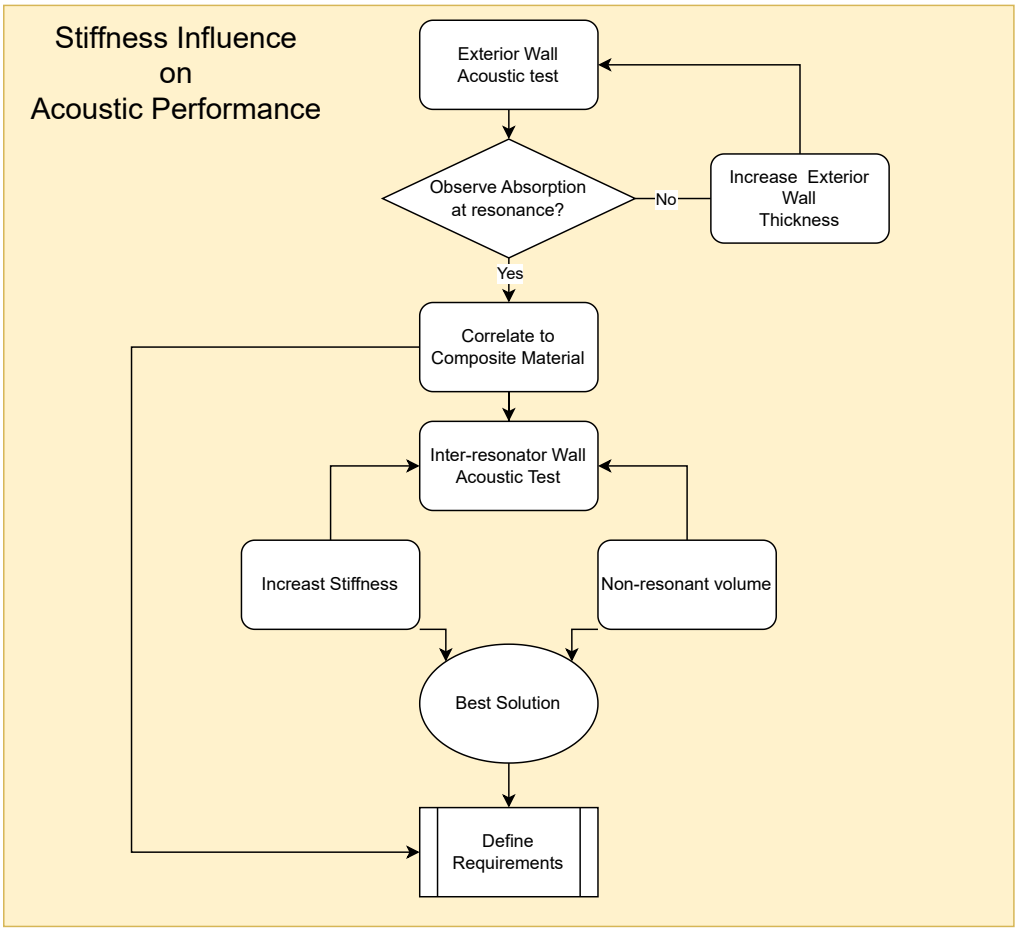

Figure 4.1: Workflow of the investigation on the influence of cell stiffness on acoustic damping.

The correlation between the 3D printed and composite material is achieved through structural stiffness equivalence. The walls were idealised as beams constrained by pin supports at both ends under an evenly distributed load, as shown in Figure 4.2. The deflection equivalence is shown in Equation 4.3. The NCAMP-certified Style 6781 S2 Glass pre-preg is used as a reference.

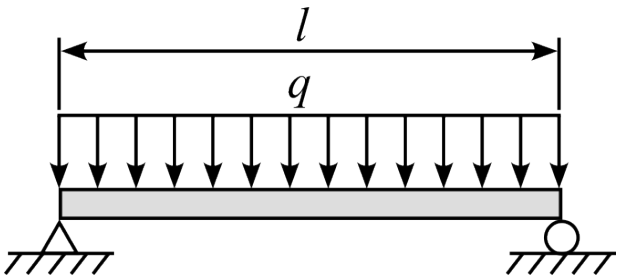

Figure 4.2: Idealised loading case for the resonator exterior walls.

$$\frac{5qL^4}{384E_{print}I_{print}} = \frac{5qL^4}{384E_{composite}I_{composite}} \tag{4.3}$$

q is the magnitude of the distributed load, L is the span, E is Young's Modulus of the material, and I is the area moment of inertia of the beam section. Since the load and span are identical for both materials, the stiffness equivalence is simplified to Equation 4.4. The printed part wall thickness corresponding to the desired composite laminate is determined such that the product between the printed samples Young's modulus and its area moment of inertia is equal to the product of the Young's modulus and area moment of inertia of the composite.

$$E_{print}I_{print} = E_{composite}I_{composite} \tag{4.4}$$

The 0.5 mm sample exhibited very high acoustic transparency, which indicates that the exterior walls of the sample were incapable of isolating the incoming sound waves. As the investigation's workflow mentioned, the sample's design was iterated upon. It was determined that a design with at least 1.5 mm of wall thickness is required to observe sound absorption at the resonance frequency. The 1.5 mm of PLA corresponds to a three-ply laminate when using the reference material.

The next step of the investigation was establishing the effect of stiffness on the interior walls of the resonator array. The first phase used the same approach, starting with a design with 0.5 mm interior walls. Figure 4.3 shows the samples tested in this investigation phase. Sample 1 is the unmodified 0.5 mm specimen, Sample 2 had its wall thickness increased to 1 mm, and Sample 3 is an alternative solution which trades resonator density for minimum weight by introducing non-resonant elements. The results of the experiments are presented in Figure 4.4. The first sample exhibited a high degree of sound transparency at the resonance frequency, closely following the contour of the ”No Sample” baseline. The second sample exhibited a much stronger absorption capability, enhancing resonance absorption. The third sample proved to be the best-performing specimen. It showed higher overall noise absorption and a much more pronounced effect at the resonance frequency.

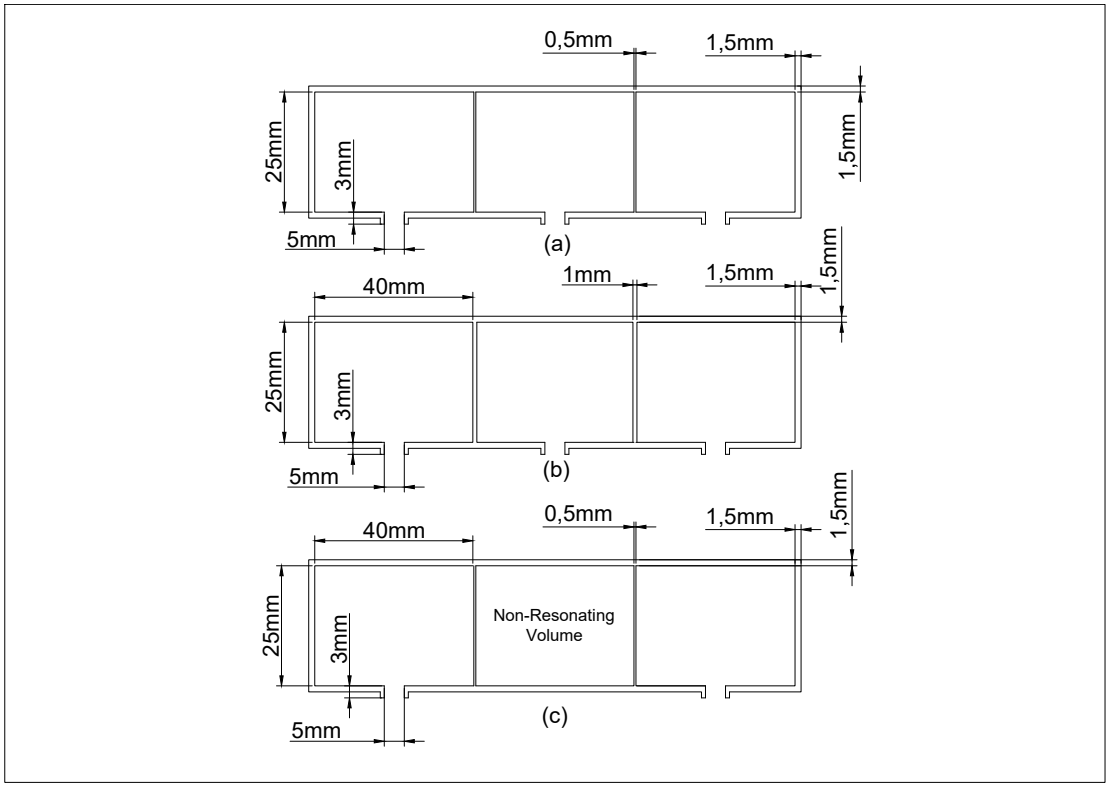

Figure 4.3: Interior wall stiffness samples. (a) Sample 1: 0.5 mm walls. (b) Sample 2: increased wall thickness from 0.5 mm to 1 mm. (c) Sample 3: 0.5mm walls and non-resonant volume in the middle.

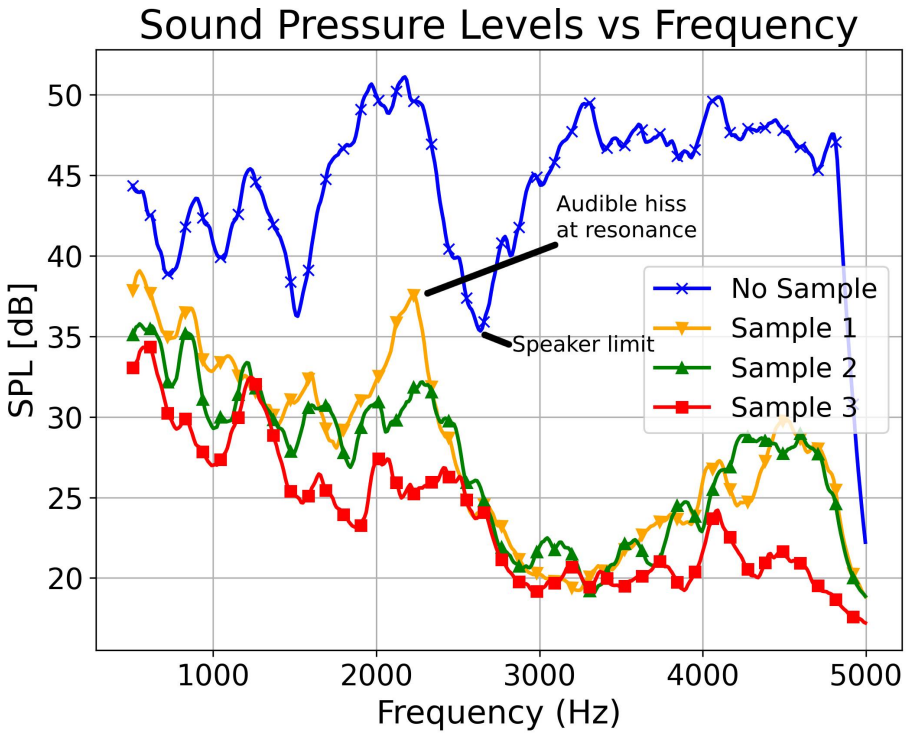

Figure 4.4: Sound level spectrum of the wall thickness samples.

The investigation concludes that the resonator's stiffness has a powerful impact on its performance. Insufficiently stiff exterior walls compromise the functionality of the resonator, while too-flexible inter-resonator walls negatively impact performance. The lightest design that is manufacturable with the available equipment cannot achieve its acoustic function. Further samples must be designed with wall thicknesses of at least 1.5 mm, and the acoustic panel core must incorporate non-resonant elements. The following acoustic panel requirements are formulated:

- The composite acoustic panel's skins shall have a lay-up that deflects less than a 1.5 mm tall plate manufactured out of PLA over a span of 40 mm under acoustic loads.
- The core of the composite acoustic panel shall incorporate non-resonant elements.

4.1.4. Influence of inlet placement on resonance frequency

The influence of placing the inlet within the resonance chamber must be established. Placing the inlet in this position is greatly beneficial from a product integration point of view. The panel's height is reduced, defined by the composite faces and core thickness, as opposed to the face sheets, core thickness and resonator inlet length. It also results in flat panels, which is beneficial from a packaging and manufacturing perspective: it facilitates the creation of tooling, storage, transportation and panel installation. This investigation workflow is presented in Figure 4.5.

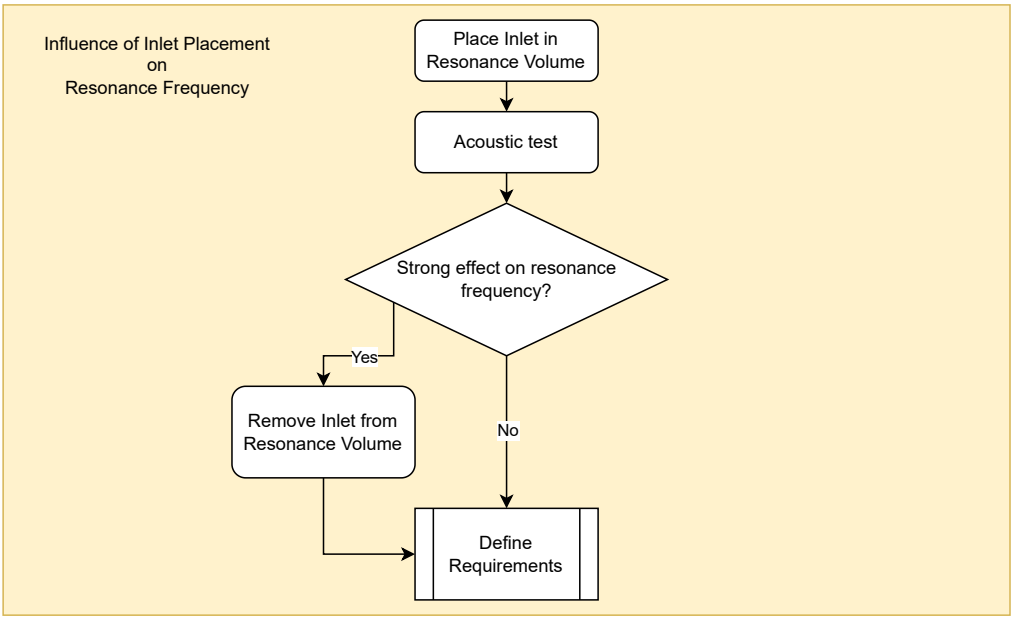

Figure 4.5: Resonator inlet placement investigation workflow.

For this investigation, five different samples were manufactured. The volume of the resonance chamber and inlet opening are constant among all samples. The inlet length varies from 2 mm to 6 mm. Figure 4.6 is a diagram of the samples. The previous findings are incorporated into the design: the resonators are manufactured with a constant wall thickness of 1.5 mm. Table 4.1 presents the geometry of the resonators and their computed resonance frequency.

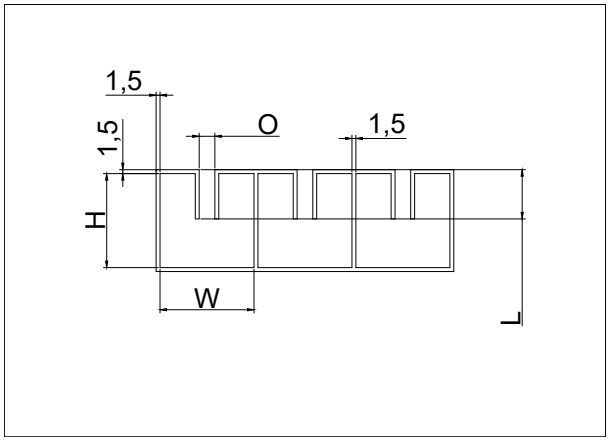

Figure 4.6: Diagram of the samples manufactured for the resonator inlet placement investigation. The section is extruded and capped at both ends to create the resonance volume and enable acoustic behaviour. H is the resonance room height. W is the resonance room width. O is the opening size. L is the length of the neck.

Item	H x W (mm x mm)	Opening 'O' (mm)	Inlet Length 'L' (mm)	F_res Comp (Hz)
Sample 1	12x12	2	2	4557
Sample 2	12x12	2	3	3736
Sample 3	12x12	2	4	3235
Sample 4	12x12	2	5	2893
Sample 5	12x12	2	6	2641

Table 4.1: Geometry data of the Helmholtz resonators used to investigate the effect of placing the neck inside the resonance chamber.

The investigation's findings are presented in Table 4.2. The samples were acoustically tested according to the presented methodology. The transmitted noise was measured, recorded, and correlated with the SPL meter to verify that sound absorption was present at the resonance frequency. The measured resonance frequency is the frequency corresponding to peak resonator absorption. No significant influence can be observed. The resonance frequency of some samples is increased while it is decreased in others. There is no observable trend. The resonance frequency increases from Sample 1 to Sample 2 and drops to a value lower than computed for Sample 3; Sample 4 shows the exact change as Sample 2, and Sample 5 shows a substantial increase. It can be concluded that the influence of the inlet placement is negligible. The following requirement is formulated:

- The resonator's inlet shall be placed within the resonance chamber as long as its length is at most 6 mm or half the height of the resonator.

Item	Inlet Length (mm)	F_res Comp (Hz)	F_res Measured (Hz)	Change (Hz)
Sample 1	2	4557	4574	20
Sample 2	3	3736	3788	42
Sample 3	4	3235	3142	-93
Sample 4	5	2893	2851	42
Sample 5	6	2641	2755	114

Table 4.2: Computed and measured resonance frequency of the inlet placement samples accompanied by the change in resonance frequency.

4.1.5. Resonator influence on failure modes

The next step in designing the lining acoustic panels is to investigate the effect of resonators on failure modes. This step is necessary, as the failure of the cabin lining poses a danger to passenger safety. Failure under gust loading can severely injure an occupant and create a feeling of panic among the rest of the passengers. Failure under crash conditions negatively impacts egress capability. Face sheet failure under tension and intracellular face sheet buckling are the most susceptible modes for cabin lining panels. This is due to the small design loads imposed on the structure: at most, 9G inertial loads are in tension, compression, or bending. The panel's face sheets carry all loads, and the small magnitude allows for thin lay-ups. Once the resonators are integrated, stability issues under compression and compromised tensile performance are experienced. The workflow of the failure mode investigation is presented in Figure 4.7.

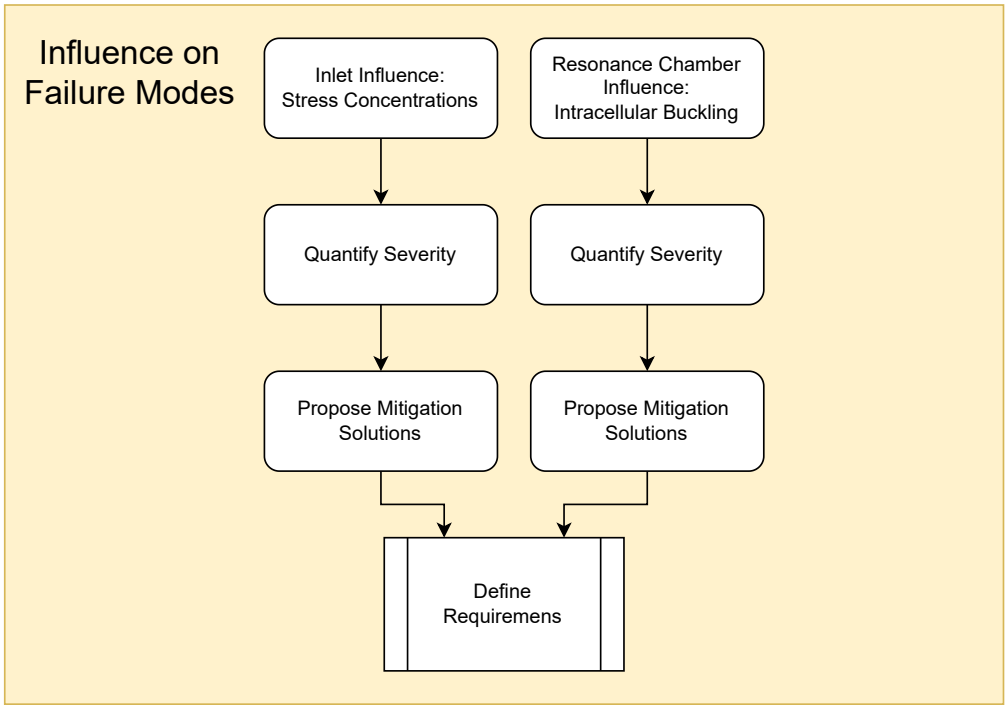

Figure 4.7: Flowchart of the failure mode investigation

The tensile load-bearing capability of the face sheets is affected by the presence of the resonator's inlet. The resonator's need to communicate with the outside environment requires using a permeable face sheet. The permeability of the face sheet is achieved through perforations matching the geometry and position of the resonator inlets. Since the material is removed, the stress flow within the panel's skin is also affected. The perforations act as stress concentrations, elevating the value of the experienced stress. Not accounting for this effect leads to the premature catastrophic failure of the component.

The investigation into the effect of the perforation idealises the problem as an elliptical hole in an infinitely large plate loaded under tension, as depicted in Figure 4.8. The material of the face sheet is assumed to be isotropic. The assumptions are valid as long as the distance between perforations in the acoustic panel is larger than five times the opening diameter, measured perpendicular to the stress flow. Treating the composite faces as isotropic material neglects the uneven loading of the composite around the openings. It is a factor that must be accounted for if such acoustic panels are integrated into current aircraft.

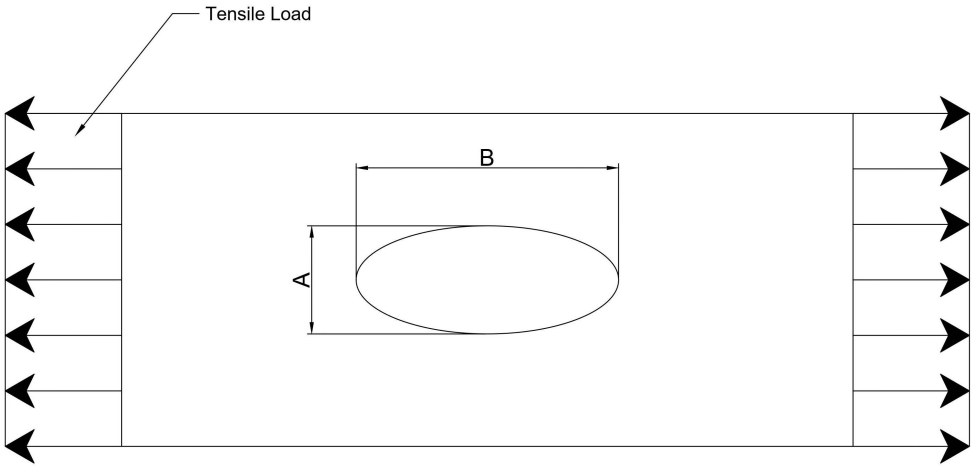

Figure 4.8: Analyseded stress concentration case

Table 4.3 shows the effect of elongating the opening. A circular hole has a stress concentration factor K of 3. Widening the opening perpendicular to the loading direction leads to a swift increase in the peak stress experienced by the component, as shown in the left columns of the table. Elongating the opening along the loading direction has the opposite effect. The peak experienced stress decreases. The effect of the openings is minimised if they are elliptical, with the semi-major axis aligned with the load path. As a result, the acoustic panel installation must constrain the edges' displacement perpendicular to the openings. Pin supports at the corners of the panel are unsuitable, as the resulting stress field under bending has components both along and perpendicular to the openings.

A/B	K	B/A	K
0.98	2,96	1,01	3,03
1,41	3,82	0,70	2,41
1,92	4,84	0,51	2,03
2,51	6,02	0,39	1,79
3,18	7,36	0,31	1,62
3,92	8,85	0,25	1,50
4,75	10,50	0,21	1,42
5,65	12,30	0,17	1,35
6,63	14,27	0,15	1,30
7,69	16,39	0,12	1,25
8,83	18,67	0,11	1,22
10,05	21,10	0,09	1,19
11,34	23,69	0,08	1,17
12,72	26,44	0,078	1,15
14,17	29,35	0,070	1,14
15,70	32,41	0,063	1,12

Table 4.3: Stress Concentration Values (K). The first two columns indicate the stress concentration values if the opening is widened perpendicular to the load applied load: A increases while B is constant. The last two columns indicate the stress concentration values for openings that are enlarged along the load path: B increases while A is constant.

The compressive stability of the face sheets is related to the honeycomb's cell size. Larger cell sizes offer less support, resulting in larger spans where buckling may occur. The introduction of Helmholtz resonators limits the design freedom of the honeycomb cell size. For a panel of a given thickness and absorption spectrum, the volume of the resonance chamber must be sufficiently large to meet the requirements defined in the previous sections and to allow for the manufacturing of the inlet and face sheet perforations.

For this investigation, a resonator is integrated into a conventional honeycomb core. The dimensions of the resonator chamber are similar to that of the samples used in the inlet position investigation. The resonator is placed in a hexagonal cell with a 12 mm inscribed circle. The height of the resonator is 12 mm. The inlet is designed according to the stress concentration investigation: it spans the cell's width. Figure 4.9 depicts the resonator cell and investigated failure mode.

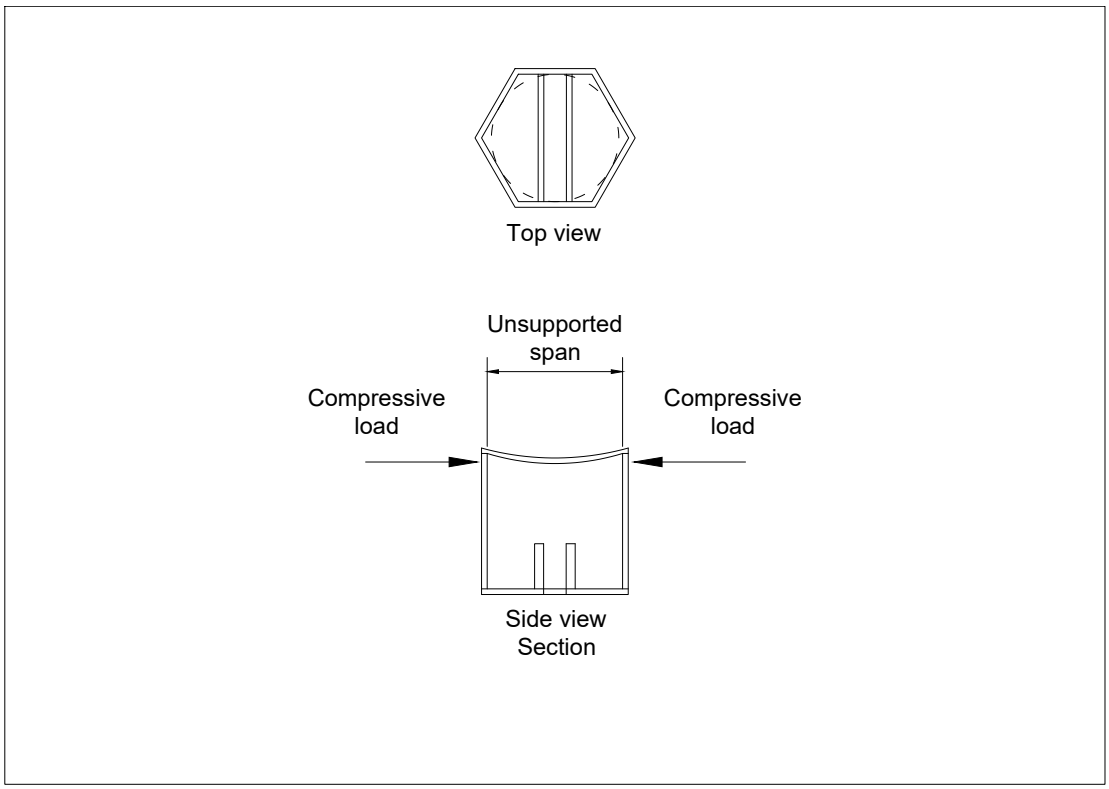

Figure 4.9: Schematic of the intracellular buckling phenomenon. The compressed face sheet of the sandwich panel buckles under compressive load within the honeycomb cell.

The resonating cell's effect on face sheet stability was analysed using the method proposed by Christos Kassapoglou [36] in his book on composite structure design. The author proposes treating the problem as Euler beam buckling instead of the more complex plate buckling situation. The difference in boundary conditions is accounted for using a semi-empirical factor. The formula for determining the intracellular buckling load is presented in Equation 4.5. D_{11} is the face sheet resistance to bending along the load path, while s is the inscribed diameter of the cell. Note that the relationship is quadratic. A doubling of the cell size reduces the buckling load by four times.

$$N_{xdim} = 24\frac{D_{11f}}{s^2} \tag{4.5}$$

The buckling load of the resonating cell is compared with commercial Nomex honeycomb cores suitable for sandwich panels with thin face sheets in Table 4.4. It can be easily observed that the cell size greatly impacts stability. The 4.8 mm honeycomb's buckling load is less than half of the 3.2 mm honeycomb's. The resonating cell has a buckling load 15 times smaller than the 3.2 mm core. A solution must be devised to increase the compressive stability of the face sheets while minimally impacting the resonator.

Material	s (mm)	Nx (N/mm)
Nomex	3.2	75.89
Nomex	4.8	33.73
Resonating cell	12	5.34

Table 4.4: Intracellular buckling load for commercial honeycomb cores and the acoustic material. The buckling load decreases exponentially with an increase in cell size.

The use of support columns is proposed to solve the issue of face sheet stability while maintaining the acoustic behaviour and resonator design freedom. Such structures are commonly used in civil engineering when elevated platforms must be constructed. Examples include airports, shopping malls, train stations, highway overpasses, glass-covered skyscrapers, and ancient structures such as the Acropolis temple in Athens. Figure 4.10 shows the support column concept. Vertical pins spanning the height of the resonator cell are placed around the resonator's inlet. The pins provide additional support, increasing the buckling load of the face sheet.

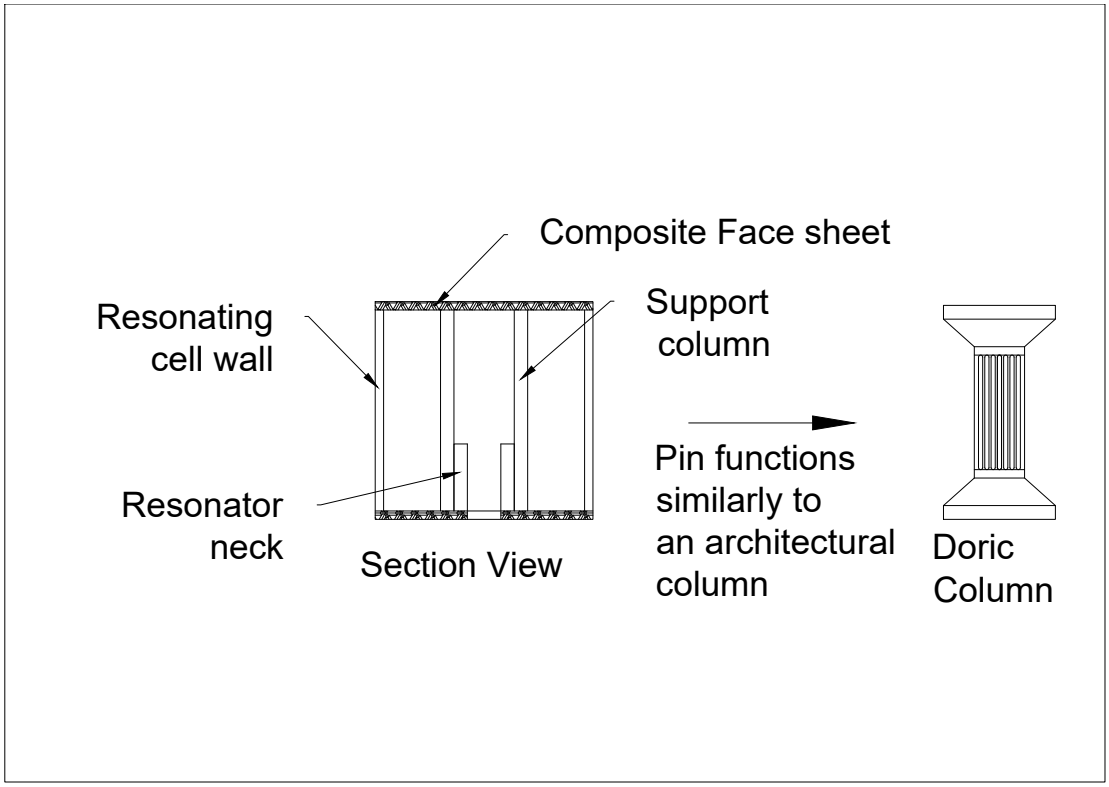

Figure 4.10: Support column concept drawing.

Figure 4.11 shows the implementation of the concept in the resonating cell and the interaction between the support column and face sheet under compressive loads. Four columns are placed near the resonator's inlet, equally spaced from the cell walls. The unsupported span is significantly reduced, resulting in a higher critical load. The solution minimally impacts the resonator's chamber while substantially increasing the load-bearing capability of the panel.

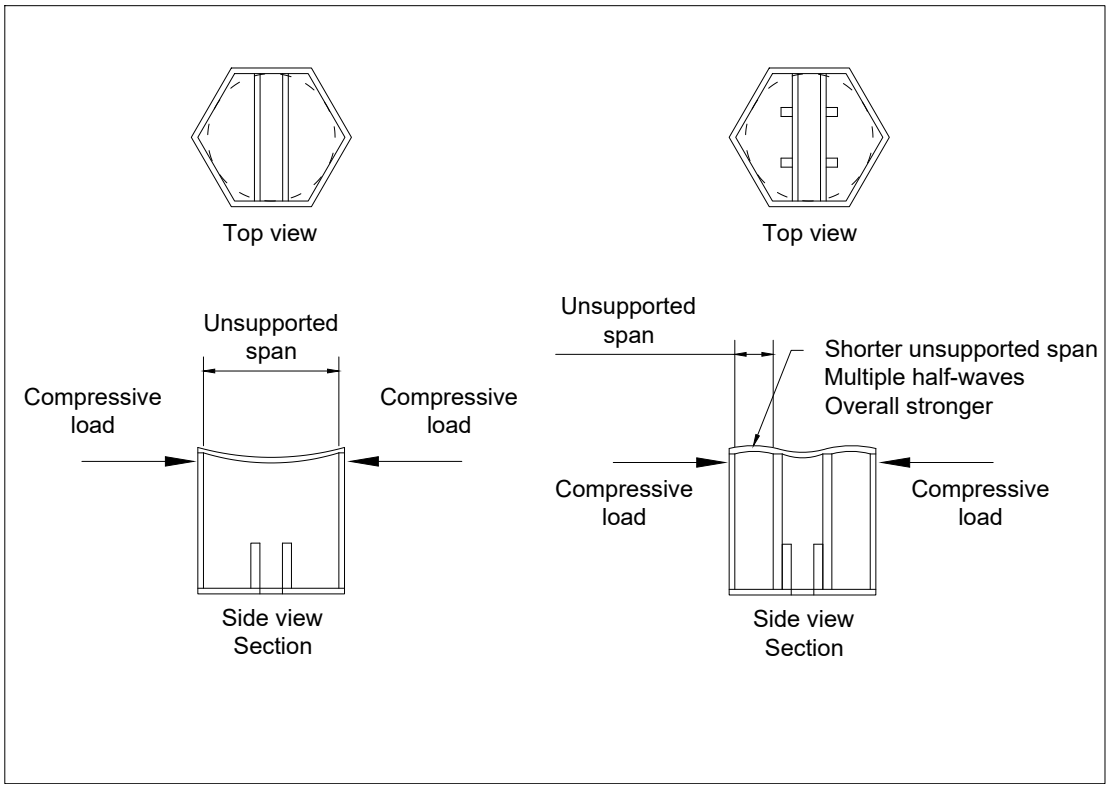

Figure 4.11: Metamaterial implementation of the support column concept.

This investigation determined that integrating resonators into honeycomb composite panels significantly impacts the load-bearing capability if the panel and resonators are improperly designed. The resonator inlets must be designed to minimise their impact on the stress field. Simultaneously, the panel's installation process and boundary conditions must be set to enforce the desired stress field: the stress flow within the face sheets shall be parallel to the resonator's inlets. The honeycomb core must also feature support columns to alleviate the stability issues experienced by the face sheets while under compression. The following design criteria are formulated:

- The resonator's inlet shall be elliptical, with the semi-major axis aligned with the stress flow.
- The installation shall allow stress to flow only parallel to the resonator inlets.
- The honeycomb core shall feature support columns placed sufficiently apart to provide the same intracellular face sheet buckling load as a honeycomb with 4 mm cells.

4.1.6. Array design

The final step in the acoustic panel's design is integrating the requirements defined by previous investigations into a functional honeycomb core. The array design focuses on determining the most suitable tesselations for resonator integration. The goal is to create a tesselation with a resonator fill ratio of at least 75%. Having a high resonator density allows for more resonators with different resonance frequencies to be integrated, increasing the absorption bandwidth of the metamaterial. The goal of 75% was set to force the array design phase of the study to minimise the size of non-resonant elements. The resonating cells follow the same definition as in the failure mode investigation: equilateral polygons defined by an inscribed circle with a diameter of 12 mm. The first step is applying the requirements to a traditional honeycomb core and determining the fill ratio. If the target is achieved, a final design has been obtained. Otherwise, additional tesselation methods are investigated. The workflow of the resonator array design is presented in Figure 4.12.

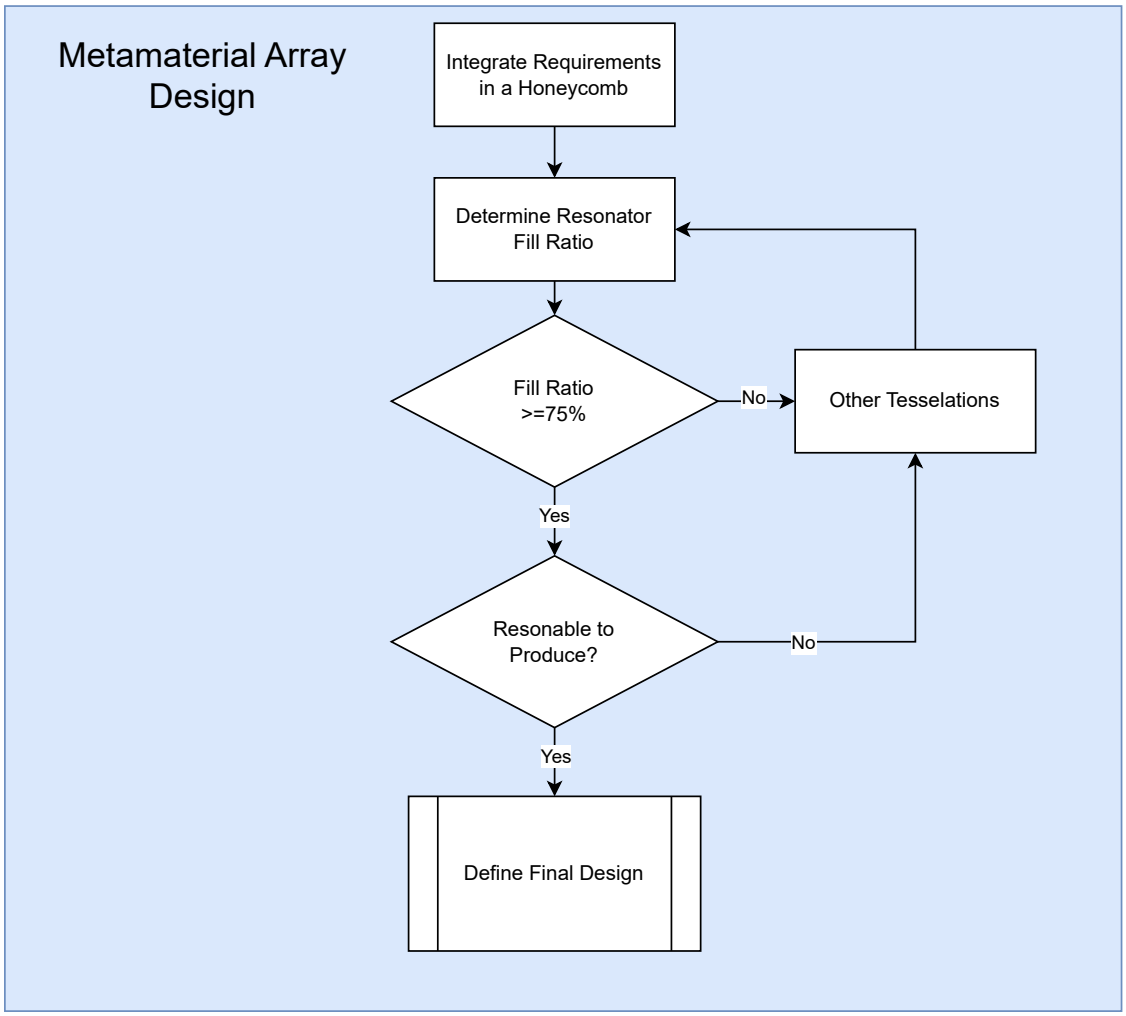

Figure 4.12: Workflow of the array design

Figure 4.13 shows a traditional honeycomb structure and resonator integration made according to the investigation performed in the first part. Due to the requirement of having non-resonant volumes between resonators, the acoustic cells are sparse, resulting in a fill ratio of 31%. Additional topologies need to be investigated. A denser resonator arrangement allows for more resonators tuned at different frequencies, thus increasing the bandwidth.

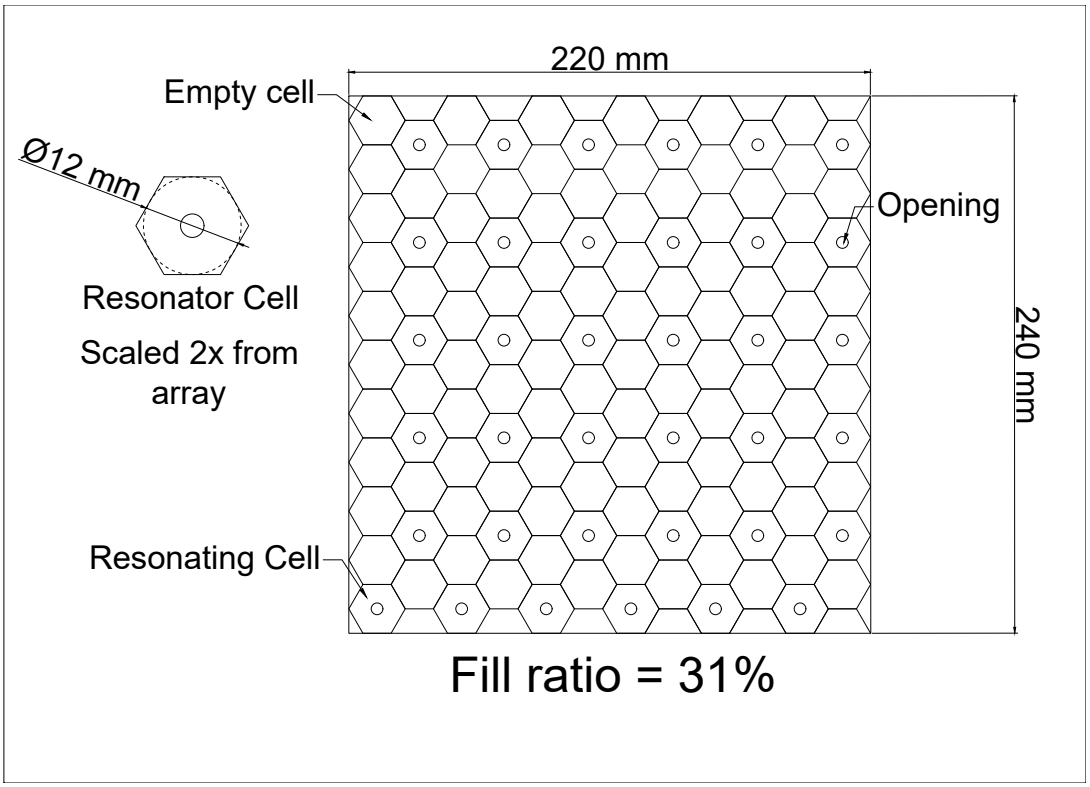

Figure 4.13: Resonators integrated into a traditional honeycomb structure according to the developed design guidelines. Many cells must remain unused, reducing the overall number of acoustic elements.

Applying a straightforward square grid design, as seen in Figure 4.14, results in more efficient packaging. Its inherent structure facilitates a heightened density of resonators. The simplicity of the square-grid configuration enables a more efficient distribution of resonating elements: the resonators are placed similarly to a chessboard. With this design, a resonator fill ratio of 50% is achieved. Although the square-grid design is more promising than the traditional honeycomb, it fails to meet the desired fill ratio.

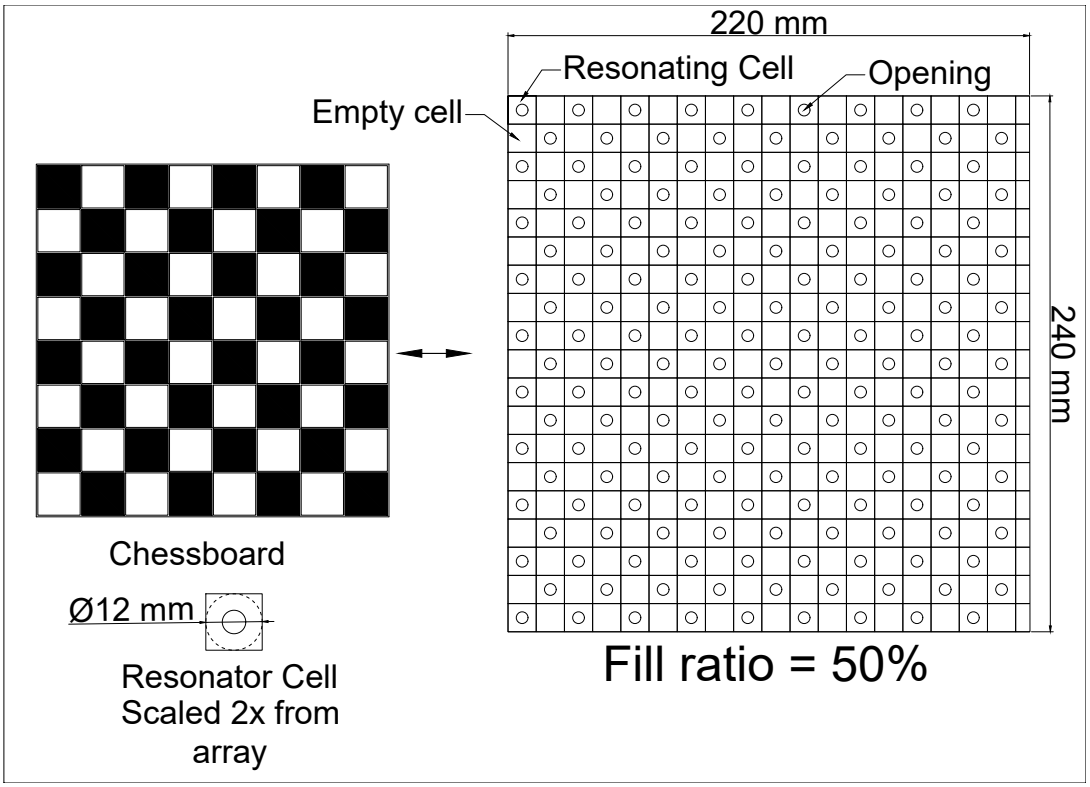

Figure 4.14: Resonators integrated into a square grid. The arrangement is created by subdividing a square into an integer number of smaller squares. The resonators are placed along lines parallel to the diagonals to avoid cross-talk. The resonators are more densely packed than the honeycomb but still present empty cells.

A tesselation combining square and hexagonal elements is presented in Figure 4.15. This arrangement's potential is cut short by a notable drawback: the large unoccupied volume around which the resonators are placed. This design is marginally better than the traditional honeycomb and less efficient than the square grid, presenting a fill ratio of 40.12%. The main drawback is the large, unused volume around which the resonators are placed.

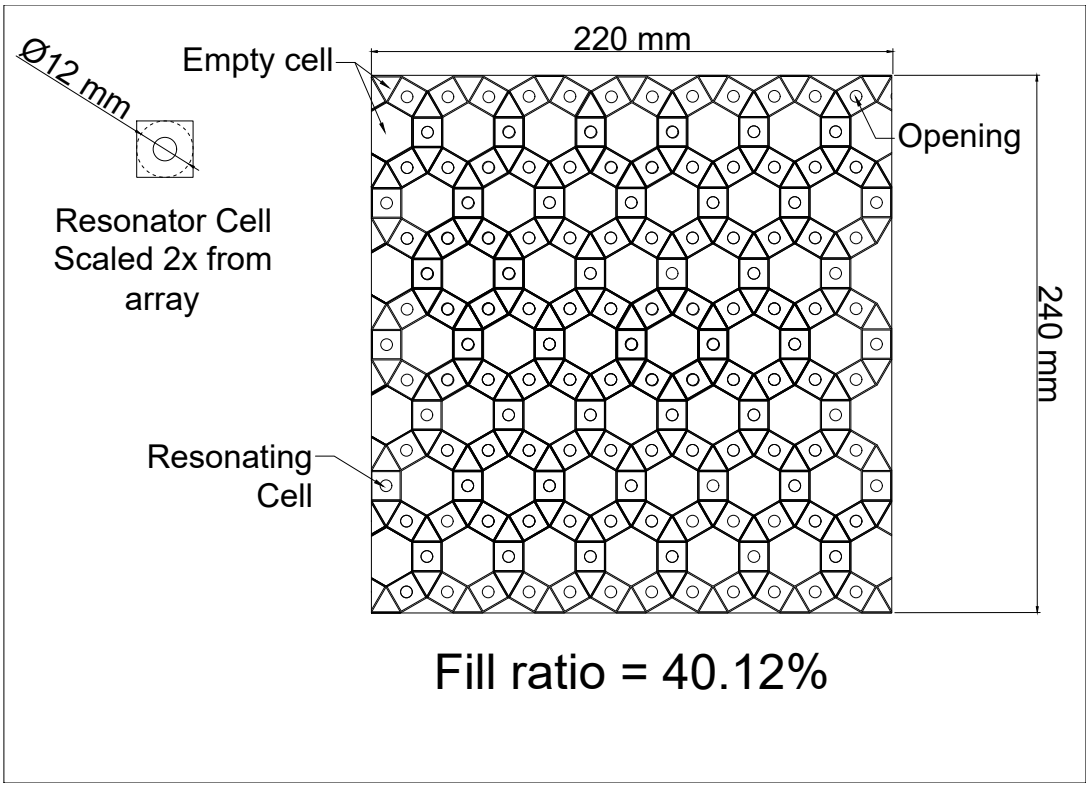

Figure 4.15: Hexagon tessellation Resonator integration. The geometry is created by arranging the resonators around the edges of a hexagon. For tessellation to be possible, the resonator volume must be cubic. Note the large, unused volume around which the resonators are placed. The unused space introduces stability issues.

The arrangement depicted in Figure 4.16 represents a different approach to isolating the resonators. Unlike previous designs that isolated the resonators by introducing non-resonant volumes, this design achieves the same effect by translating the honeycomb cells along their edges until contact is maintained only at the corners. This approach produces a topology comprising hexagons and triangles, leading to a stiffer geometry than the previous options. Furthermore, the resonator density is significantly increased, reaching a fill ratio of 75%. This topology is used for the acoustic panel's core.

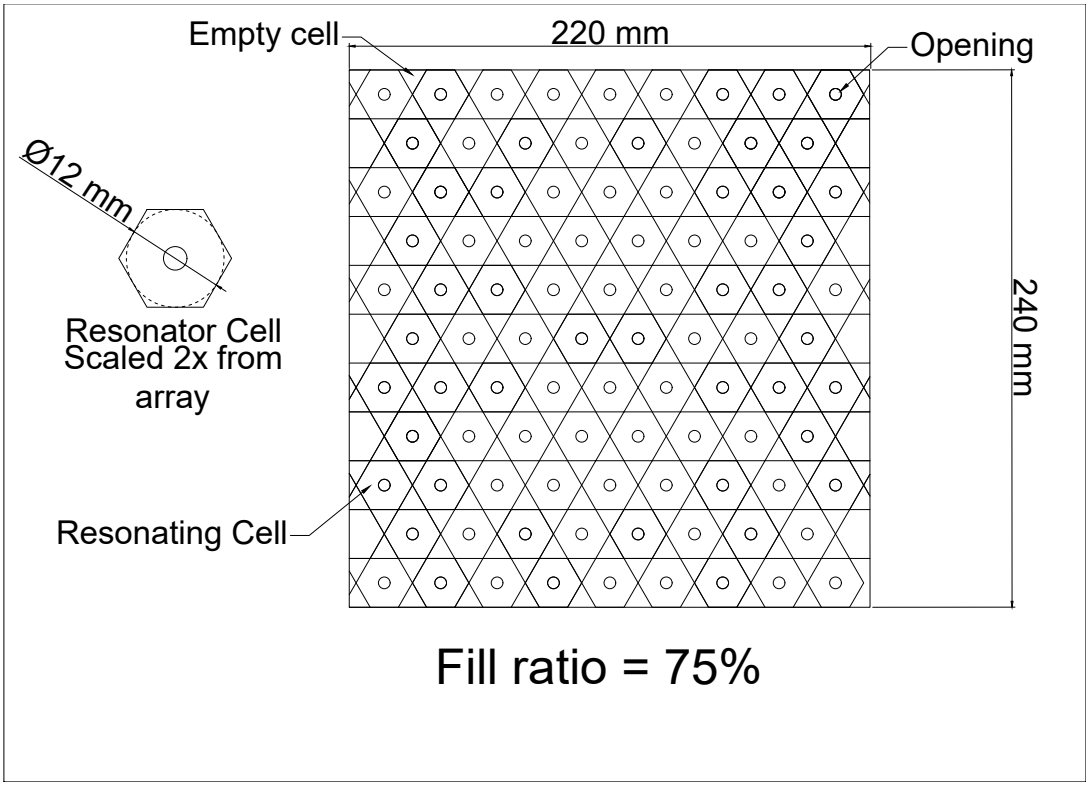

Figure 4.16: Offset Honeycomb Resonator integration. The geometry is created by offsetting the cells of a honeycomb so that contact is maintained only at the corners. This arrangement allows for a much higher resonator density than the previously presented options. The empty cells are much smaller than the previous designs and triangular in section. The result is a stiffer topology.

4.2. Final design

The final resonating core design is presented in Figure 4.17. It is an offset honeycomb geometry with 12 mm resonating cells. The openings measure 2 mm wide and cover the distance between opposite sides of the unit cell. The thickness of the core is 12 mm. Two different resonators were integrated into this design: one at 3500 Hz and one at 4000 Hz. The difference in resonance frequency is achieved through different inlet lengths: 3.5 mm and 4.5 mm. The anti-buckling pins were also incorporated to verify if they interfered with the resonator functionality. A detailed view of the resonating unit cell can be seen in Figure 4.18. The design was modified to allow for tiling. Doing so allows for creating panels larger than the 3D printer's work area. Interlocking elements were added around the perimeter of the metamaterial. A cyanoacrylate adhesive is used to secure the tiles when creating larger cores.

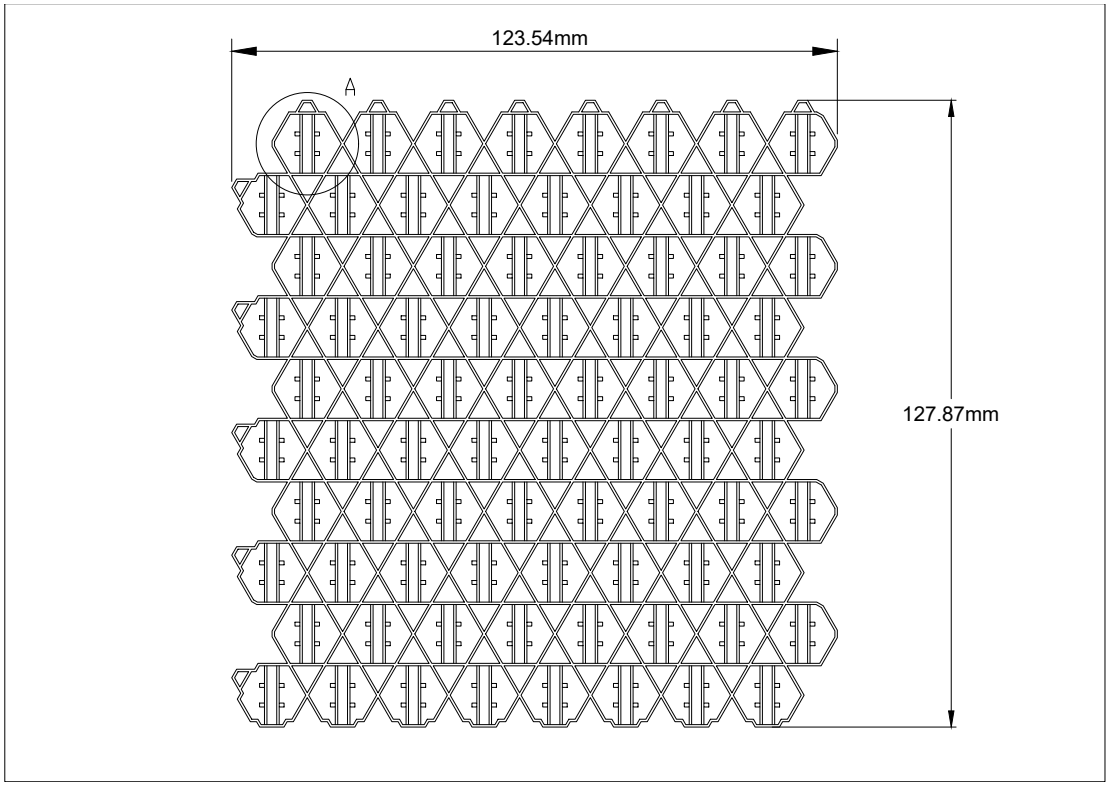

Figure 4.17: CAD drawing of the metamaterial core. The sample has an overall dimension of 123.54 x 127.87 mm or ten rows of 8 resonating cells. The trapezoidal geometry on the top and left edges was added to facilitate the creation of surfaces larger than the printer bed. Thickness is 12 mm.

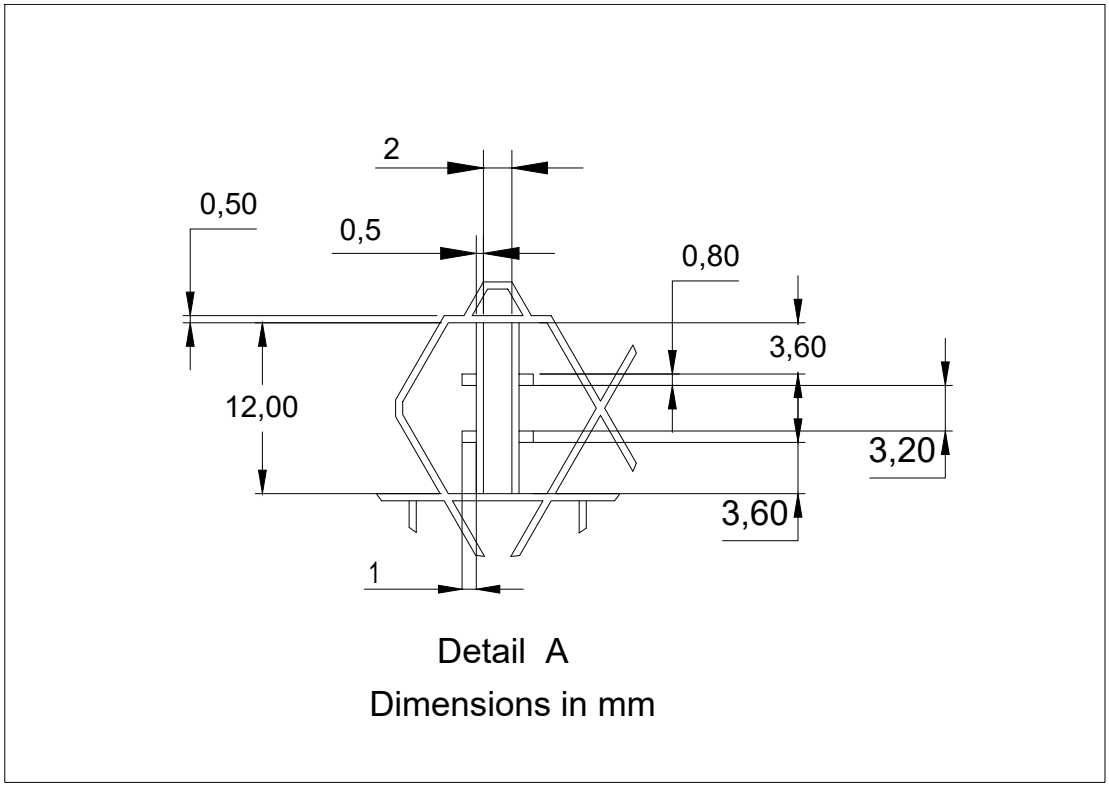

Figure 4.18: Detail A of Figure 4.17. Geometry parameters relevant to the acoustic element. The cell size measures 12 mm between parallel sides. The opening is 2 mm wide and spans from the cell's top to the bottom walls. The wall thickness of the metamaterial is 0.5 mm. The anti-buckling pins are 0.8 x 1 mm. The resonance frequency is controlled by varying the neck length.

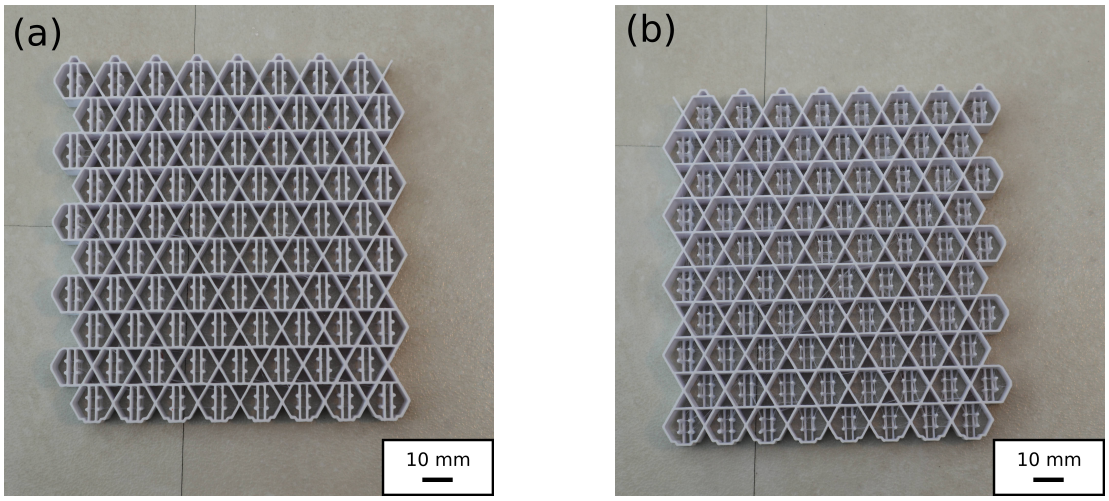

Figure 4.19: Manufactured core using FDM in PLA. (a) fuselage facing side, with the resonator opening. (b) cabin facing side.

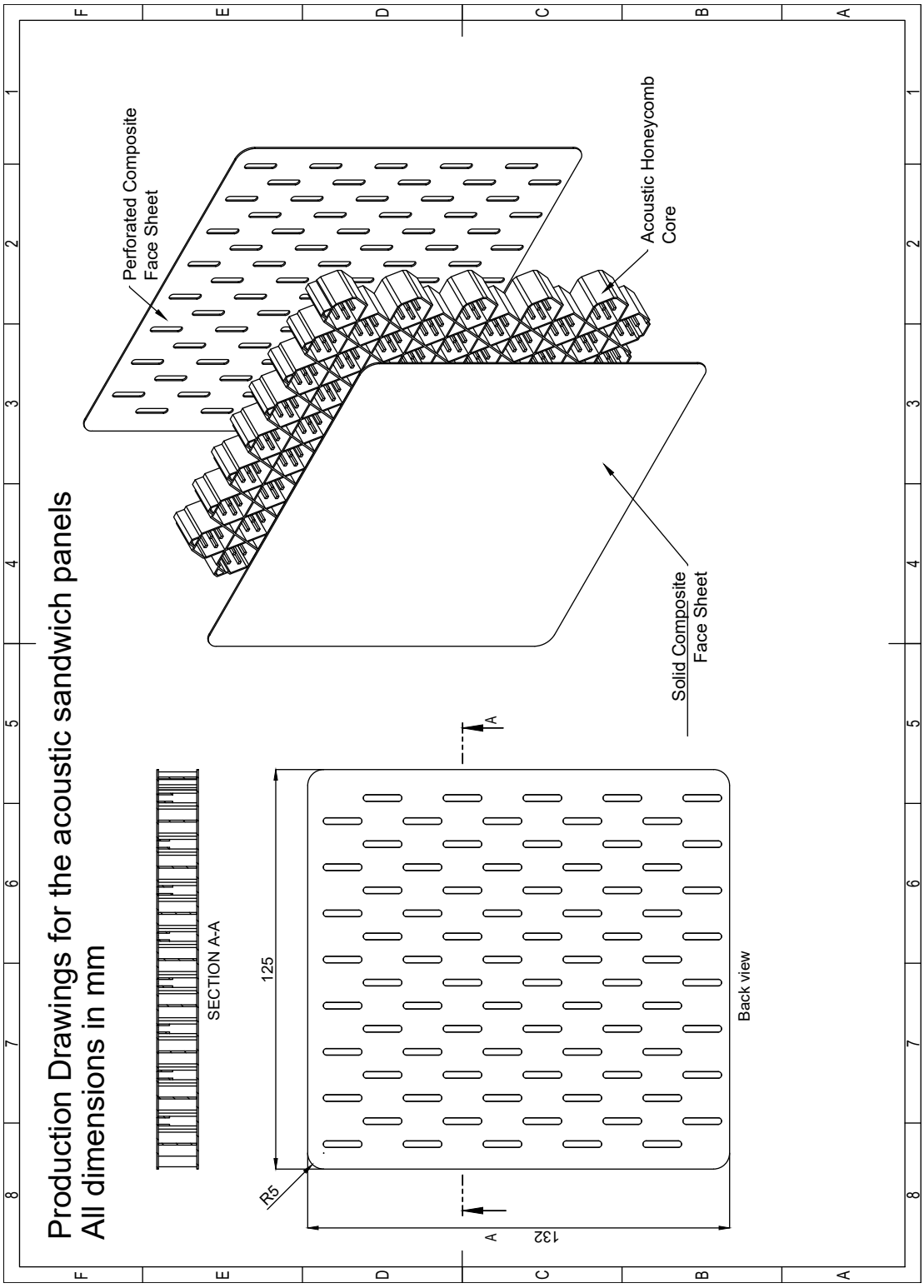

Figure 4.20: Production drawings of the small acoustic sandwich panels.

4.2.1. Discussion on Fabrics, filters and opening obstructions

Helmholtz resonators rely on open volume, resulting in a susceptibility to dust and debris. Additional dust and debris were observed in the oldest test samples. Intrusions within the resonance chamber reduce the available volume and influence wave propagation unpredictably. A filtration system must be implemented to safeguard the functionality of the metamaterial regardless of cleanliness.

A pragmatic solution was devised to address this concern. A 1.15 mm thick wool cloth with a 415 g/m^2 density was placed atop the resonator openings. This fabric layer is an effective filter, shielding the resonator from contamination. The choice of a thicker and heavier fabric is deliberate. It accounts for the gradual accumulation of particulate matter over the operational lifespan of an aircraft. This measure preserves the functionality of the metamaterial and does not require additional attention from maintenance crews. The filters can be replaced or cleaned if desired.

4.2.2. Material suitability & Design validation

This section presents the work on material suitability and design validation. The honeycomb core presented in Figure 4.17 is integrated into three composite sandwich panels with differing reinforcement fibres. Fibreglass, carbon fibre and flax fibre are the three materials whose suitability for acoustic panels is investigated. The composite skins and sandwich panels are manufactured according to the process described in Chapter 3. The acoustic panel's sound absorption capability is measured using the same setup used in the design process. Figure 4.21 presents the workflow used in this section.

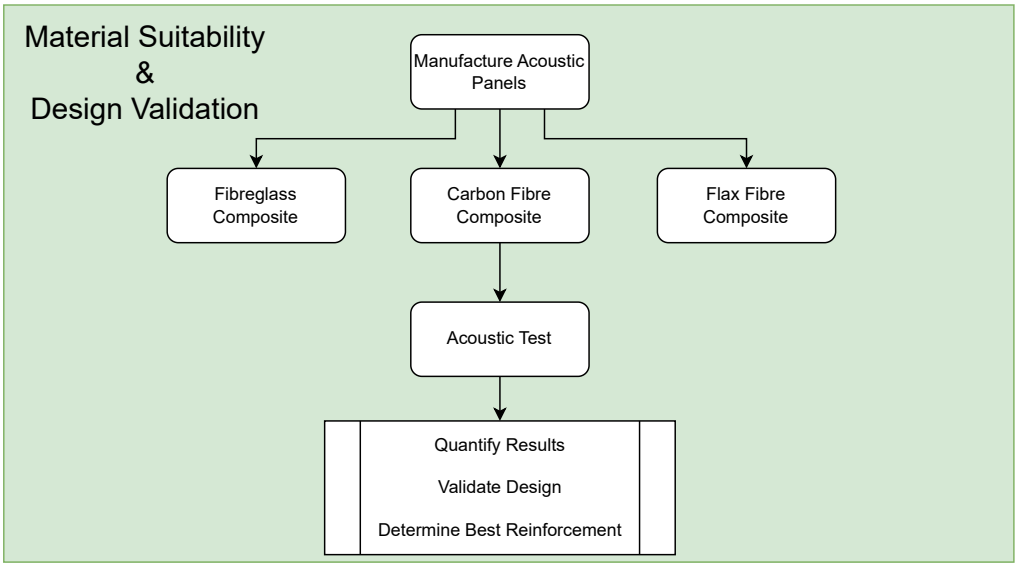

Figure 4.21: Flowchart of the work on material suitability and design validation.

Figure 4.22 to Figure 4.24 show the manufactured samples. Although there are minor imperfections, such as slight misalignments between the resonator slits in the face sheet and their corresponding channels in the core, their impact on the resonators is minimal. Factors like temperature and pressure differences influence resonating frequency more than slight alignment errors. The cloth was attached using double-sided tape. The hole in the fabric Does not affect the acoustic setup. It sits away from the opening of the acoustic enclosure.

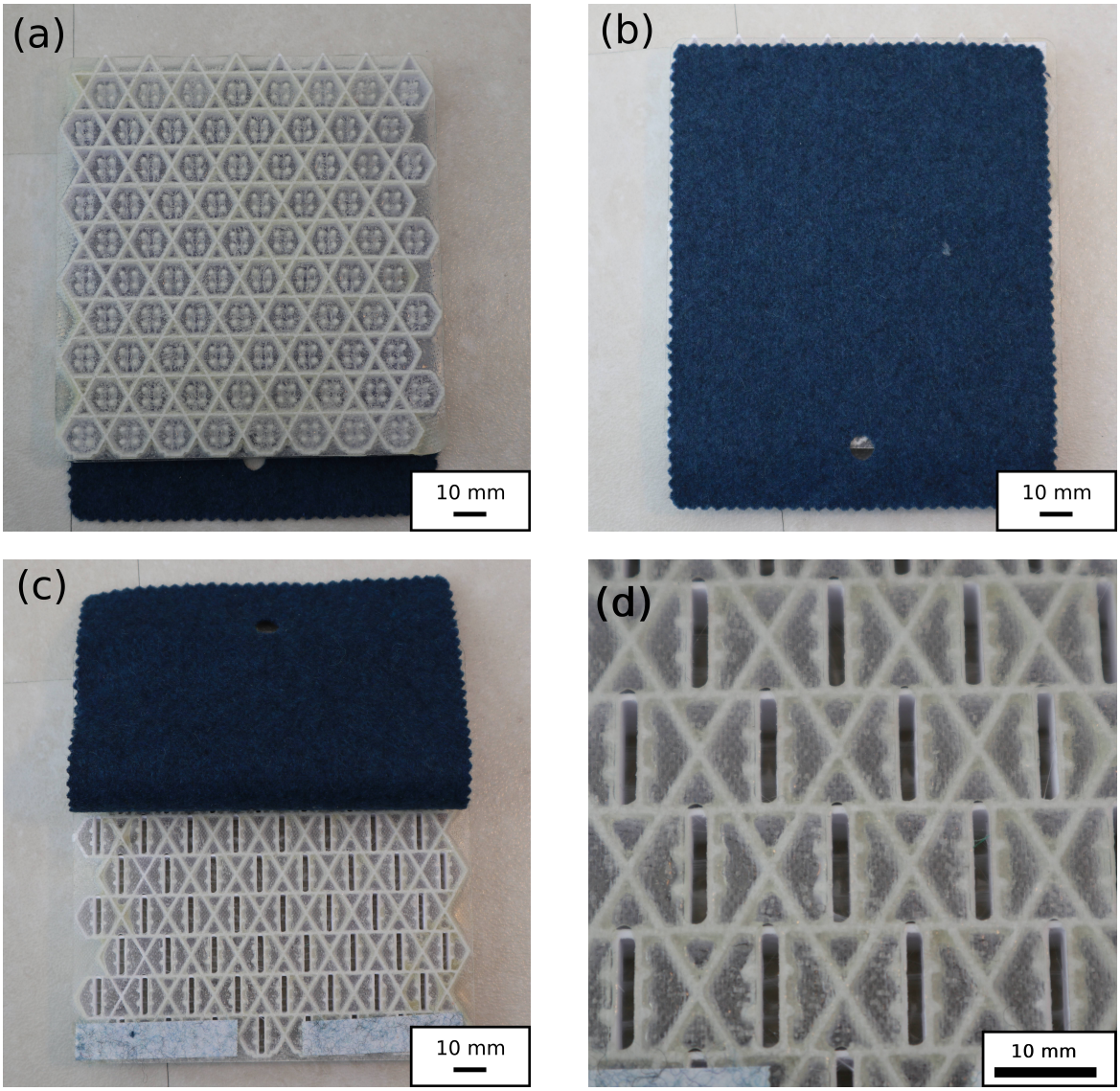

Figure 4.22: Fibreglass composite acoustic test specimen. (a) Front face. (b) Back face, with cloth. (c) Back face without cloth. (d) Close-up of resonator inlets.

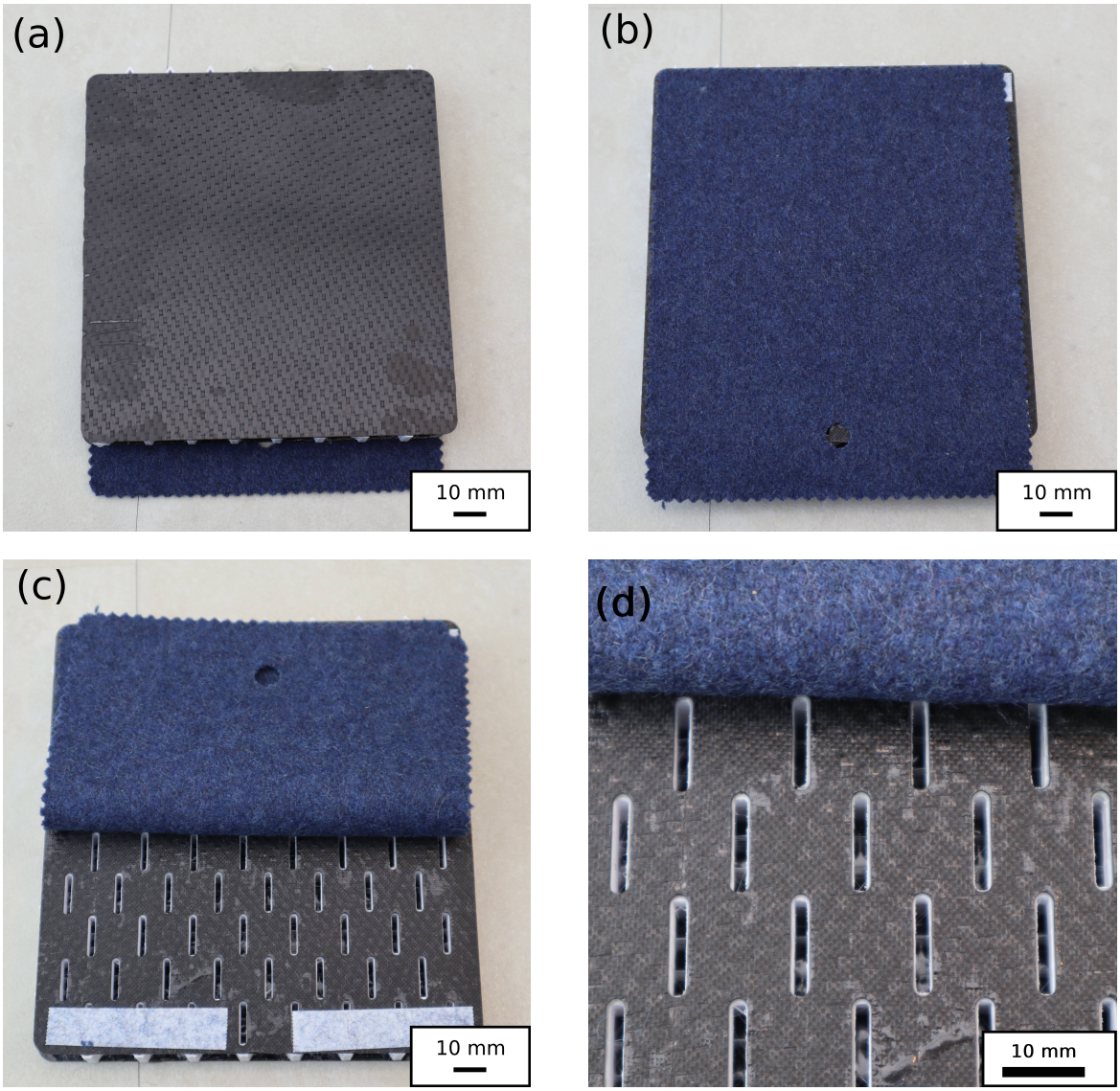

Figure 4.23: Carbon fibre composite acoustic test specimen. (a) Front face. (b) Back face, with cloth. (c) Back face without cloth. (d) Close-up of resonator inlets.

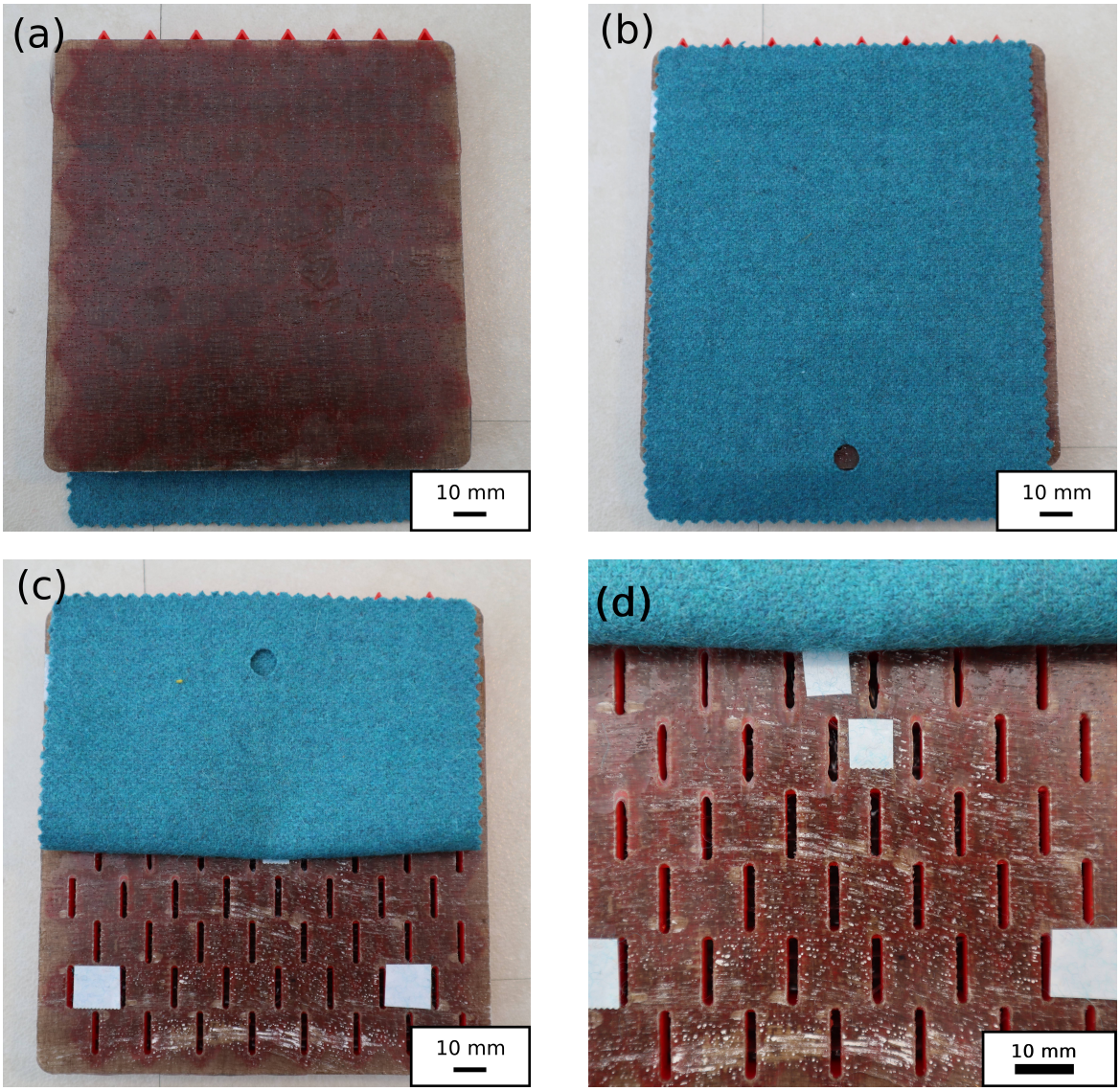

Figure 4.24: Flax fibre composite acoustic test specimen. (a) Front face. (b) Back face, with cloth. (c) Back face without cloth. (d) Close-up of resonator inlets.

A comparative approach was used to assess sound absorption performance accurately, evaluating the panels relative to a reference sample devoid of resonating elements. This reference sample, marked as blank, provides a baseline for determining the effectiveness of the panels in absorbing sound energy across different frequencies. Figure 4.25 is the spectral breakdown of the sound pressure level. To better visualise the sample's performance, the difference in sound levels between the samples and "No Sample" condition (Figure 4.26) and the metamaterial and blank (Figure 4.27) are plotted. Finally, the absorption coefficient is determined by computing the emitted and transmitted acoustic power ratio (Figure 4.28).

The design requirements defined in this thesis have proven to be effective. The samples demonstrate elevated absorption levels around the resonance frequency of the Helmholtz resonators when compared with the blank sample, as illustrated best in Figure 4.26. Each of the three samples exhibits a peak in absorption around 3500 and 4000 Hz. Additionally, the anti-buckling pins do not show any noticeable effect on the metamaterial's performance.

Next, the performance of various face sheet materials is analysed. It was observed that fibreglass was the most effective, followed by flax and carbon fibre trailing last. The efficacy of each face sheet reinforcement can be best observed in Figure 4.27. The difference in performance is suspected to be due to each laminate's mechanical properties, indicating that the stiffness issue is much more complex than initially assumed. The fibreglass and flax composite have similar Young's modulus, while the carbon fibre is much stiffer. The specifications of the face sheets can be seen in Table 4.5. The size of the resonance cells is also tiny, making estimations of the behaviour even more difficult. The distance between supports can be measured in multiples of fibre tows. The same issues with estimating the buckling behaviour within the resonance cells are also present in this case: the scale is too close to that of the fabric and lamina levels.

Reinforcement	Thickness	Lay-up	Fabric weave
Fibreglass	0.5	[0/90]t	8HS
Carbon fibre	0.5	[0/90]t	2x2 Twill
Flax fibre	1.5	[0/90]t	UD

Table 4.5: Faces sheet specifications.

Finally, it was observed that the effect of the metamaterial is not limited to only the tuned resonant frequency, but it also presents integer multiples. The samples show increased absorption at frequencies up to three times lower than the tuning target. The observed behaviour allows for high absorption at lower frequencies without drastically changing resonators or adding mass through traditional solutions. Figure 4.28 best depicts the phenomenon. The blank sample is substantially less absorbent than the other three in the 1500 - 2000 Hz range, corresponding to half of the resonant frequency of the metamaterial.

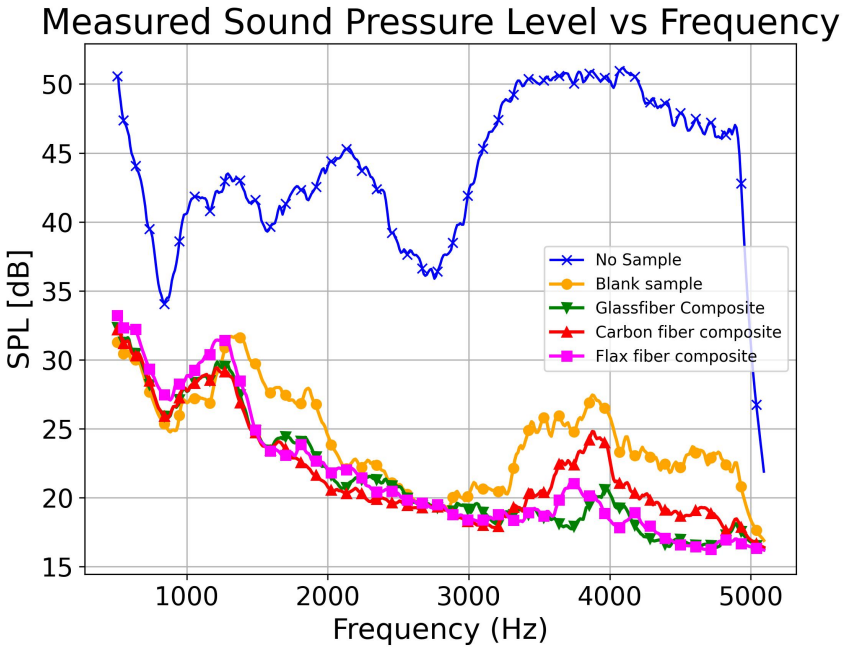

Figure 4.25: SPL spectrum plot. In the resonance range of the metamaterial (3500-4000 Hz), the measured sound levels are below the blank sample (no resonators)

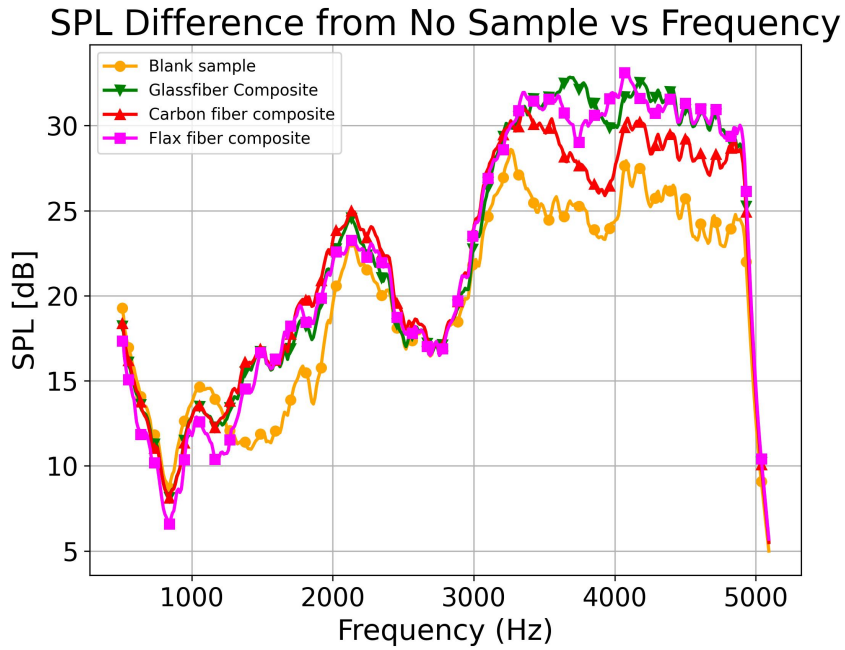

Figure 4.26: Drop in Sound Pressure Levels from the No Sample condition. The fibreglass and flax fibre composites reach a reduction of up to 33 dB. The fibreglass composite is more consistent. The carbon fibre composite trail behind, reaching a peak reduction of 30 dB. The blank sample is visibly outperformed.

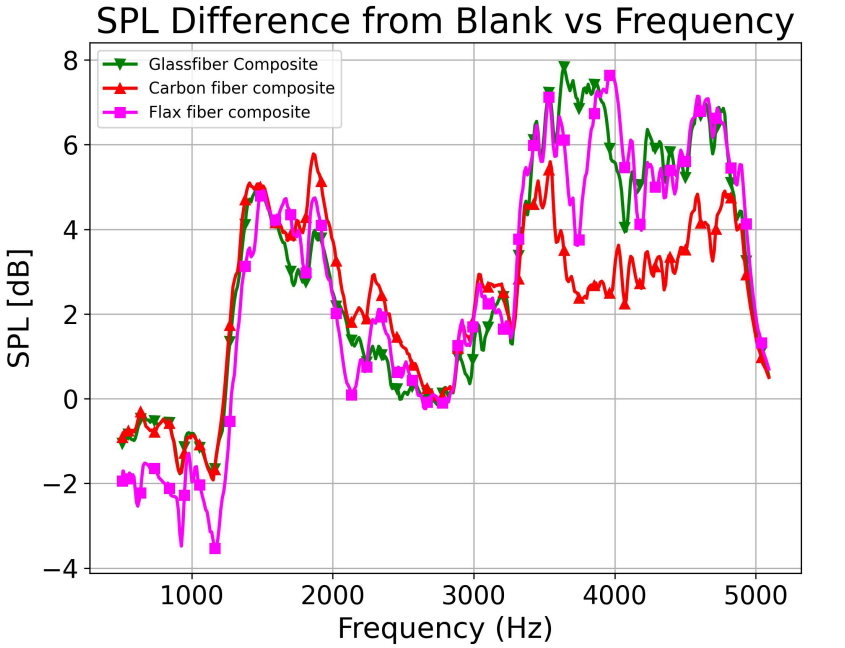

Figure 4.27: Difference in SPL Levels between the resonating and non-resonating sample. The fibreglass composite is the highest performing, followed by the flax composite, reaching an 8 dB reduction in noise levels. The carbon fibre composite is less effective, peaking at 5 dB, followed by a steep decline to 2 dB.

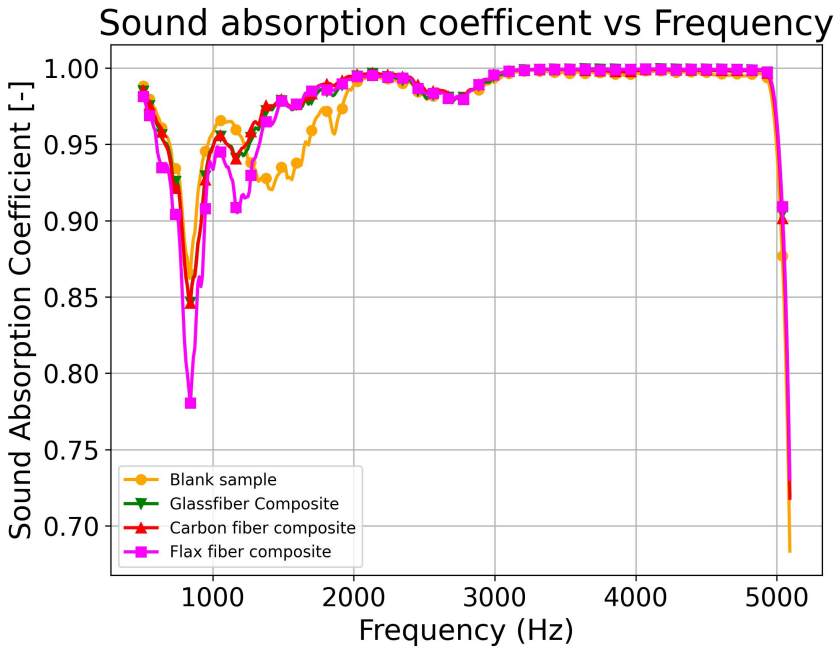

Figure 4.28: Absorption coefficient of the composite samples. In the resonance range, the absorption coefficient is very similar. The difference in the percentage of absorbed noise power is minimal. Interestingly, the increased absorption coefficient of the composite samples in the 1500-2000 Hz region is one octave lower than the metamaterial's tuning. The metamaterial is effective at multiples of its base resonance.

4.2.3. Acoustic panel weight analysis

The final step of the research is to investigate the weight of the acoustic panels and determine potential weight-saving avenues. The manufactured acoustic panels are weighed, and a breakdown of the mass of each component is generated. The mass of the core is extracted from the slicing software. The mass of the core is compared with commercial honeycomb offerings to determine the mass difference between the developed acoustic panel and a standard sandwich panel manufactured with the same techniques. The mass breakdown is then used to determine which elements of the core's design and manufacturing process need further improvements to reduce the final weight of the acoustic panel. A workflow of the analysis performed in this chapter is presented in Figure 4.29.

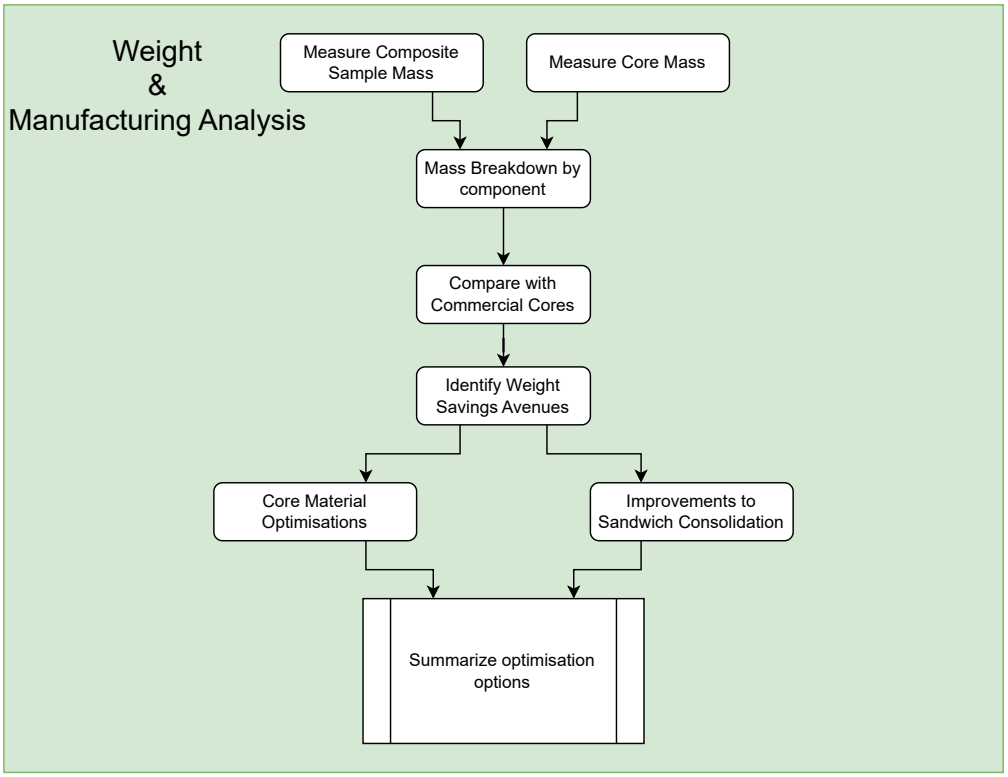

Figure 4.29: Acoustic panel weight analysis flowchart.

Table 4.6 presents the mass of the three samples and a mass breakdown. The mass of the core is extracted from the slicing software. The combined weight of the face sheets and adhesive is determined through differentiation. The areal density of each sample is computed by dividing its mass by its surface area.

Sample	Total Mass (g)	Face Sheets + Adhesive (g)	Core Mass (g)	Areal weight (g/m^2)
Fibreglass composite	98	45	53	5947
Carbon fibre composite	99	46	53	6007
Flax fibre composite	103	50	53	6250

Table 4.6: Sample weight breakdown and areal density of the samples. The total weight was determined using a kitchen scale. The core weight was extracted from the slicing software. The core's weight was subtracted to determine the face sheets and adhesive mass.

The primary limitation is the minimum extrusion width for the FDM process. The printer features a nozzle of 0.4 mm. A wall thickness of at least 0.5 mm was required to maintain consistency between model iterations and avoid issues with the slicing software and bed adhesion. These restrictions resulted in samples with areal weights of 3.35 kg/m^2. Table 4.7 compares various commercial honeycomb cores. The core developed and manufactured using the current process is too heavy. A smaller nozzle diameter, such as 0.2 mm, offers a 50% weight reduction potential. Self-foaming polymers, such as the various available lightweight PLA formulations, could provide further weight reduction.

Material	Cell size (mm)	Thickness (mm)	Areal Weight (g/m^2)
Nomex	3.2	12	368
Al	3.2	12	865
Al	19.1	12	345
Metamaterial	12	12	3350

Table 4.7: Density comparison between various commercial honeycomb cores and the developed metamaterial for a thickness of 12 mm. The metamaterial developed through FDM is heavier in order of magnitude.

Another avenue is improving the secondary bonding step by using dedicated adhesive films or relying on a single consolidation process, resulting in a complete panel. The first option focuses on strictly controlling the amount of adhesive used, while the second step foregoes adding material for potentially more complexity at other stages of the process: cutting of the resonator slits needs to be done on each ply of the yet-to-be-consolidated fabric or the finished product. Pre-forming the slits scales with the number of plies used and adds time, while machining the openings at the end damages the material, causing local delaminations at the edges of the slits.

Finally, breaking down the generated topology by function sheds light on another potential weight-reduction solution. The walls of the resonators, more specifically, hexagon tessellation, serve as load-bearing structures and barriers between resonators. The neck of the resonators defines the resonance frequency and enables acoustic behaviour. Isolating the neck and pins in a separate component, as seen in Figure 4.30, allows for a disconnect in terms of material and manufacturing. The hexagonal tessellation can be made out of Nomex paper, which is around five times thinner and has a similar density to the PLA used in this project. The resonator neck can be redefined as an Acoustic Enabling Device (AED), which weighs around 0.2 g/part, totalling 1.3 kg/m^2 in the final design. Implementing these proposed changes results in an acoustic metamaterial with an areal density of 1.7 kg/m^2 for a thickness of 12 mm. The challenges with the proposed solution are creating the cutting and folding pattern to obtain the desired tessellation and accurately placing the AEDs.

4.2.4. Manufacturability analysis

The acoustic panel's manufacturability was evaluated through the production process of the samples used to determine material suitability. Two additional panels, larger than the acoustic test specimens, were used to gauge the scaling potential of the process used in this research. The resonator inlets have the most substantial impact. Additional time was spent creating the necessary perforations, and a dedicated tool (Figure 3.2) was made to spread adhesive while not plugging the inlets. Manufacturing the metamaterial core is also one of the points that needs improvement. The core of the small samples weighs only 53 grams, yet it has a print time of over three hours. The large samples are made out of nine smaller cores tiled together. The total print time for one large panel is 31.5 hours. Additive manufacturing is not suitable due to the time investment required. The methods proposed for weight reduction may improve the manufacturing process. Splitting the metamaterial into a conventional core and AEDs allows the core and resonator elements to be produced separately. Using adhesive films may remove the need for the adhesive spreading jig. A method for creating the panel in a single consolidation phase is more desirable. The perforations need to be made on a pre-impregnated fabric.

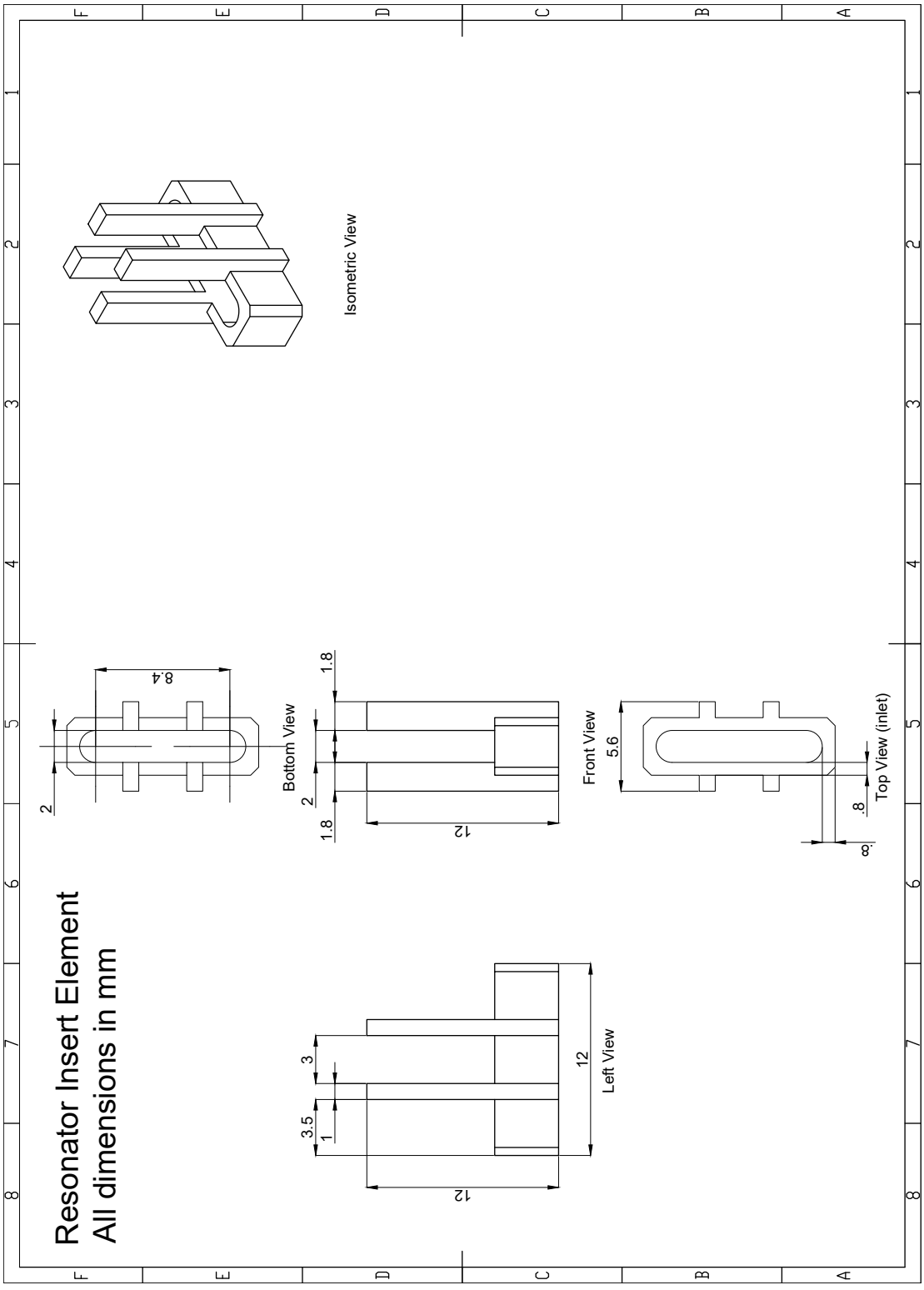

Figure 4.30: Acoustic Enabling Device (AED) concept: This device allows any honeycomb to be acoustically enhanced as long as the insert can be manufactured to fit the desired cell size and resonance frequency.

5

Conclusion

The thesis addresses the research question by proposing an innovative acoustic panel incorporating resonating cells within a composite sandwich structure. The novel design efficiently separates the acoustic and structural elements, with stress impacts limited to the resonator openings in the outer layers. It is achieved by embedding the resonators entirely within the panel's core. Unlike existing aviation acoustic panels, which utilise two layers for the resonator inlet and resonating chamber, this new approach enables the creation of single-layer resonating panels, promising lighter and thinner structures without compromising acoustic and mechanical performance.

The following requirements need to be defined to develop Helmholtz resonator-based metamaterials suitable for use as core materials in lightweight composite sandwich structures:

1. The composite acoustic panel's skins shall deflect less than a 1.5 mm tall plate manufactured out of PLA over a span of 40 mm under acoustic loads.
2. The core of the composite acoustic panel shall incorporate non-resonant elements. Corner contact between the resonators is allowed. Common edges are to be avoided.
3. The resonator's inlet shall be placed within the resonance chamber as long as its length is at most 6 mm or half the height of the resonator.
4. The resonator's inlet shall be elliptical, with the semi-major axis aligned with the stress flow.
5. The installation shall allow stress to flow only parallel to the resonator inlets.
6. The honeycomb core shall feature support columns placed sufficiently apart to provide the same intracellular face sheet buckling load as a honeycomb with 4 mm cells.

The investigative and design process led to the development of a novel composite acoustic panel. This panel comprises a core with non-permeable skin on one side and permeable skin on the other. The core incorporates a honeycomb structure with integrated ducts and support columns, significantly enhancing the panel's sound absorption capabilities by creating a cavity within the core cells and the skins. The honeycomb structure's cells are arranged to have only corner contact, maximising the presence of resonators in the panel. The integrated ducts enable the panels to remain flat, while the support columns improve structural performance under compressive loads by preventing buckling within the core cells.

Developing this innovative composite acoustic panel with integrated resonating cells represents a significant advancement in structural acoustic engineering. The ability to create single-layer resonating panels that are lighter and thinner without compromising performance has far-reaching implications for aerospace and other industries. This study addresses the research question and lays the groundwork for future composite acoustic panel technology innovations.

6

Recommendations for future research

This chapter outlines recommendations for future work to enhance the applicability of the results and deepen the understanding of the performance of phononic metamaterials in structural applications.

Limitations of the current research

Like much of the literature, the current study primarily focuses on acoustics. The developed phononic panel is not mechanically characterised, and its elastic properties and failure modes remain unknown. The proposed solutions, such as support columns to counteract intracellular buckling, have not been investigated for efficacy. Additionally, the effect of stricter boundary conditions has been neglected: stiffer connections between components may serve as more efficient sound transmission paths. Comprehensive characterisation of the metamaterial and investigation into the implications of implementing resonant phononic panels in aircraft structures is essential.

Future research directions

Future research should focus on the following key areas to advance the understanding and application of phononic metamaterials in structural applications:

Structural recommendations

A study is required to establish the panel's failure loads and the ideal resonator opening geometry. For this study, it was chosen to minimise the number of plies needed per face at the cost of stricter boundary conditions. The attachment methods are also undefined, with the only specification being "constraining the stress flow in the panel parallel to the resonator inlets". Due to the connection between flanking and the panel's structural performance, a single study should simultaneously focus on both recommendations: first, establishing a trend for the attachment stiffness and acoustic performance, and then determining panel specification: opening geometry and face sheet stacking to reach the lowest possible weight.

Acoustic recommendations

The primary recommendation for future research from an acoustic point of view is to perform a test campaign at the component level instead of the coupon level presented in this report. It has been proven that implementing Helmholtz resonators into a sandwich panel is possible and offers increased sound reduction when the openings are pointed toward the noise source. The stricter boundary conditions imposed by the inlets and the continuous support of the edges perpendicular to the openings influence the flanking paths. Reducing the amount of noise passing through the material is pointless if another transmission path is facilitated.

Further research could involve architected geometries with viscoelastic behaviour to better counteract flanking. Improvements in the attachment methods also translate to flat panels, enabling larger cabins by allowing more efficient load transfer.

References

[1] Werner S Weiglhofer et al. *Introduction to complex mediums for optics and electromagnetics*. Vol. 123. SPIE Press, 2003.

[2] T.J. Cui et al. In: *Metamaterials: Theory, Design, and Applications* (Jan. 2010). DOI: 10.1007/978-1-4419-0573-4.

[3] Viktor G Veselago. "THE ELECTRODYNAMICS OF SUBSTANCES WITH SIMULTANEOUSLY NEGATIVE VALUES OF AND μ". In: *Soviet Physics Uspekhi* 10.4 (Apr. 1968), p. 509. DOI: 10.1070/PU1968v010n04ABEH003699. URL: https://dx.doi.org/10.1070/PU1968v010n04ABEH003699.

[4] J. B. Pendry. "Negative Refraction Makes a Perfect Lens". In: *Phys. Rev. Lett.* 85 (18 Oct. 2000), pp. 3966–3969. DOI: 10.1103/PhysRevLett.85.3966. URL: https://link.aps.org/doi/10.1103/PhysRevLett.85.3966.

[5] John Wilby. "Aircraft Cabin Noise and Vibration Prediction and Passive Control". In: Apr. 2008, pp. 1197–1206. DOI: 10.1002/9780470209707.ch99.

[6] G. Mathur et al. "Md-90 cabin noise diagnostics ground and flight tests". In: *5th AIAA/CEAS Aeroacoustics Conference and Exhibit*. DOI: 10.2514/6.1999-1834. eprint: https://arc.aiaa.org/doi/pdf/10.2514/6.1999-1834. URL: https://arc.aiaa.org/doi/abs/10.2514/6.1999-1834.

[7] W.V. Bhat et al. "Interior noise radiated by an airplane fuselage subjected to turbulent boundary layer excitation and evaluation of noise reduction treatments". In: *Journal of Sound and Vibration* 18.4 (1971), pp. 449–464. DOI: https://doi.org/10.1016/0022-460X(71)90097-6. URL: https://www.sciencedirect.com/science/article/pii/0022460X71900976.

[8] Heow Pueh Lee et al. "Assessment of in-cabin noise of wide-body aircrafts". In: *Applied Acoustics* 194 (2022), p. 108809.

[9] V Jayachandran et al. "Piezoelectrically driven speakers for active aircraft interior noise suppression". In: *Applied Acoustics* 57.3 (1999), pp. 263–277. DOI: https://doi.org/10.1016/S0003-682X(98)00056-5. URL: https://www.sciencedirect.com/science/article/pii/S0003682X98000565.

[10] C. Guigou et al. "CONTROL OF AIRCRAFT INTERIOR BROADBAND NOISE WITH FOAM-PVDF SMART SKIN". In: *Journal of Sound and Vibration* 220.3 (1999), pp. 541–557. DOI: https://doi.org/10.1006/jsvi.1998.1972. URL: https://www.sciencedirect.com/science/article/pii/S0022460X98919721.

[11] Jun Mei et al. "Dark acoustic metamaterials as super absorbers for low-frequency sound". In: *Nature communications* 3.1 (2012), p. 756.

[12] Kai Pang et al. "Highly efficient cellular acoustic absorber of graphene ultrathin drums". In: *Advanced Materials* 34.14 (2022), p. 2103740. DOI: 10.1002/adma.202103740.

[13] Ni Sui et al. "A lightweight yet sound-proof honeycomb acoustic metamaterial". In: *Applied Physics Letters* 106.17 (2015), p. 171905. DOI: 10.1063/1.4919235.

[14] Chuanmin Chen et al. "Hybrid acousto-elastic metamaterials for simultaneous control of low-frequency sound and Vibration". In: *Journal of Applied Physics* 129.5 (2021), p. 054902. DOI: 10.1063/5.0028332.

[15] Nansha Gao et al. "Low frequency acoustic properties of a honeycomb-silicone rubber acoustic metamaterial". In: *Modern Physics Letters B* 31.11 (2017), p. 1750118. DOI: 10.1142/s0217984917501184.

[16] Gang Yong Song et al. "Broadband fractal acoustic metamaterials for low-frequency sound attenuation". In: *Applied Physics Letters* 109.13 (2016), p. 131901. DOI: 10.1063/1.4963347.

[17] Nansha Gao et al. “Elastic wave modulation of double-leaf abh beam embedded mass oscillator”. In: *Applied Acoustics* 173 (2021), p. 107694. DOI: 10.1016/j.apacoust.2020.107694.

[18] Nansha Gao et al. “Complex band structure and Evanescent Bloch wave propagation of periodic nested acoustic Black Hole Phononic Structure”. In: *Applied Acoustics* 177 (2021), p. 107906. DOI: 10.1016/j.apacoust.2020.107906.

[19] Nansha Gao et al. “Low-frequency elastic wave attenuation in a composite acoustic black hole beam”. In: *Applied Acoustics* 154 (2019), pp. 68–76. DOI: 10.1016/j.apacoust.2019.04.029.

[20] Jie Deng et al. “Broad band gaps for flexural wave manipulation in plates with embedded periodic strip acoustic black holes”. In: *International Journal of Solids and Structures* 224 (2021), p. 111043. DOI: 10.1016/j.ijsolstr.2021.111043.

[21] Philip A. Feurtado et al. “Transmission loss of plates with embedded acoustic black holes”. In: *The Journal of the Acoustical Society of America* 142.3 (2017), pp. 1390–1398. DOI: 10.1121/1.5001503.

[22] Zixian Liang et al. “Extreme acoustic metamaterial by coiling up space”. In: *Physical review letters* 108.11 (2012), p. 114301.

[23] Zhe Chen et al. “An open-structure sound insulator against low-frequency and wide-band acoustic waves”. In: *Applied Physics Express* 8.10 (2015), p. 107301.

[24] Yu Liu et al. “Fractal acoustic metamaterials with subwavelength and broadband sound insulation”. In: *Shock and Vibration* 2019 (2019).

[25] H. Q. Nguyen et al. “A Fano-based acoustic metamaterial for ultra-broadband sound barriers”. In: *Proceedings of the Royal Society A: Mathematical, Physical and Engineering Sciences* 477.2248 (2021). DOI: 10.1098/rspa.2021.0024.

[26] CHIEN EUGENE et al. *ACOUSTIC PANELS COMPRISING LARGE SECONDARY CAVITIES TO ATTENUATE LOW FREQUENCIES*. Nov. 2017. URL: https://worldwide.espacenet.com/patent/search/family/058387704/publication/EP3244038A1?q=EP3244038A1.

[27] Yufan Tang et al. “Hybrid acoustic metamaterial as super absorber for broadband low-frequency sound”. In: *Scientific Reports* 7.1 (2017), pp. 1–11.

[28] Sibo Huang et al. “Acoustic perfect absorbers via Helmholtz resonators with embedded apertures”. In: *The Journal of the Acoustical Society of America* 145.1 (2019), pp. 254–262.

[29] Junfei Li et al. “A sound absorbing metasurface with coupled resonators”. In: *Applied Physics Letters* 109.9 (2016), p. 091908.

[30] Augusto Carvalho De Sousa et al. “Parallel assembly of acoustic resonators to obtain narrow-band unity sound absorption peaks below 1000 HZ”. In: *http://www. icedyn. net/* (2019).

[31] Giuseppe Catapane et al. “Coiled quarter wavelength resonators for low-frequency sound absorption under plane wave and diffuse acoustic field excitations”. In: *Applied Acoustics* 209 (2023), p. 109402.

[32] Yi Fang et al. “Acoustic metaporous layer with composite structures for perfect and quasi-omnidirectional sound absorption”. In: *Composite Structures* 223 (2019), p. 110948.

[33] Abhishek Gautam et al. “On the acoustic performance of double degree of freedom helmholtz resonator based acoustic liners”. In: *Applied Acoustics* 191 (2022), p. 108661.

[34] Ahmad Yusuf Ismail et al. “Sound transmission loss of a Helmholtz Resonator-based acoustic metasurface”. In: *Applied Acoustics* 188 (2022), p. 108569.

[35] Taehwa Lee et al. “Damped resonance for broadband acoustic absorption in one-port and two-port systems”. In: *Scientific reports* 9.1 (2019), p. 13077.

[36] Christos Kassapoglou. *Design and analysis of composite structures: with applications to aerospace structures*. John Wiley & Sons, 2013.